Title
RELATIVISTIC HEAVY ION REACTIONS

Author
Poskanzer, A.M.

Publication Date
1977-08-01

Invited paper presented at the
International Conference on
Nuclear Structure, Tokyo, Japan,
September 5 - 10, 1977

LBL-6586 c.1

RELATIVISTIC HEAVY ION REACTIONS

Arthur M. Poskanzer

August 1977

Prepared for the U. S. Energy Research and
Development Administration under Contract W-7405-ENG-48

INVITED PAPER FOR THE INTERNATIONAL CONFERENCE ON NUCLEAR STRUCTURE,
Tokyo, September 5-10, 1977

RELATIVISTIC HEAVY ION REACTIONS

Arthur M. Poskanzer
Nuclear Science Division
Lawrence Berkeley Laboratory
University of California
Berkeley, California 94720 USA

ABSTRACT

The present status of the study of central collisions of relativistic heavy ions is presented. The phenomenology is described and evidence is presented for a source of nucleons from a central region caused by the overlapping densities of the target and projectile. Some of the current theoretical approaches are described including the nuclear fireball model. It appears that there is a quasi-equilibrated region at high temperature, but the signature for the expected effects of high density is not yet clear, and therefore, experimentally, the effects of high density have not been identified.

The Bevalac (Fig. 1) is a combination of two accelerators. The first is the SuperHILAC, a linear accelerator for heavy ions up to 8.5 MeV/nucleon. The second is the Bevatron, a synchrotron whose output energy can be varied from 150 MeV/nucleon up to about 2 GeV/nucleon, that is, velocities ranging from 0.5 c to 0.9 c. At present the heaviest projectile with good intensities for counter experiments is ^{40}Ar.

What do we expect to see from the interaction of relativistic heavy ions with heavy target nuclei? In Fig. 2 is shown a schematic of such a reaction. We can classify reactions as peripheral or central. In a peripheral interaction we expect to see groups of nucleons clearly associated with the target and projectile. In more central collisions, because of the fast transit time of the projectile compared to the nuclear relaxation time, we may expect a localized region with extreme values of excitation energy and density. This leads to the concept of spectators and participants.[1] Thus we may expect that there will be nucleons from the target spectator, the projectile spectator (if the impact parameter is large enough), but most importantly, nucleons which participate in the initial energy and momentum transfer which are mutually swept out from the target and projectile. In Fig. 3 we see a peripheral interaction,[2] that is, two groups of nucleons clearly separated from each other in velocity and angle. The study of projectile fragmentation in such reactions has reached a mature state[3] and will not be emphasized here. In Fig. 4 you see a head-on collision of an Ar nucleus at 1.8 GeV/nucleon with a lead target.[4] Many charged particles are emitted. This is the kind of collision which is just beginning to be explored experimentally and with many different theoretical approaches;

it will be the main subject discussed here. The multiplicity of charged particle tracks[4] in such collisions is shown in Fig. 5 to range up to 100. This happens to be the sum of the number of protons in the target plus projectile, even though some of the tracks must be pions and some composite nuclei.

What do we expect to learn from such horrendously complicated collisions that we could not learn from the simple study of high energy protons on hydrogen or the study of low energy heavy ion reactions? Our goal is to study nuclear matter at high density and temperature. The binding energy of nuclear matter as a function of density is shown[5] in Fig. 6; the derivative of this curve with respect to density is the equation of state. What is known experimentally about nuclear matter at present is one point, that is, the equilibrium density of nuclei, and the binding energy of nuclear matter. Also, we know that at this point there is a minimum; nuclei are bound. Even the curvature at this point, that is, the compressibility is not known experimentally. The various curves are speculations about what might happen at high density, such as the abnormal nuclear matter of Lee and Wick,[6] or pion condensation which has been discussed in the preceding paper.[7]

The present central collision experiments at the Bevalac are of two kinds: a) exclusive measurements, with emulsions, track detectors, or the streamer chamber, and b) single particle inclusive measurements with counter telescopes or magnetic spectrometers. The first kind have more information content per event, but are difficult to analyze and have poorer statistics. The second kind give complete information on the energy spectra and angular distribution of a single fragment from an event. However, these measurements are now also being supplemented by measurements of the multiplicity of other fragments in each event.

Our counter telescope study of central collisions is oriented to observe the participants, that is, nucleons and pions from the initial density overlap with velocity intermediate between that of the target and projectile and with large transverse momentum.[8] It is a collaborative project between LBL, GSI, and Marburg University. Our scattering chamber which is shown in the upper part of Fig. 7 is one meter in diameter with 3 mm-thick walls, containing a ΔE-E telescope, and surrounded by 80 plastic scintillators. The scintillators measure the associated multiplicity of charged particles of any kind, above a low energy threshold, in coincidence with one fragment which is identified in the telescope and has its energy and angle measured. Therefore, we measure single particle inclusive spectra with associated multiplicity. The bottom of Fig. 7 shows a projected view of the scintillators looking down the beam line. Since we record the data event by event, we are able to obtain the visual displays shown in Fig. 8 for three events: a) a peripheral event, b) a central collision, and c) a rather asymmetrical event. One simple thing to extract from the data is the average multiplicity of charged particles which penetrate the wall of the scattering chamber, that is, with energies greater than 25 MeV/nucleon. These average multiplicities, corrected for the missing solid angle, are plotted in Fig. 9 for all the projectile, target combinations we have studied. The abscissa is the multiplicity of participant protons predicted by the geometrical model where the nuclei make clean, cylindrical cuts through each other, as shown in Fig. 2. The calculated number of participant protons, averaged over all impact parameters, is the number of protons in the target nucleus times the area of the projectile nucleus, plus the number of protons in the projectile nucleus times the area of the target nucleus.[9] This is divided by the total reaction cross section to obtain the expected multiplicity. In this approximation pions are neglected and it is assumed that each charged fragment contains only one proton. The solid lines are at 45° through the origin. The 400 MeV/nucleon data fit nicely on the line, but the 1.05 GeV nucleon data are high. This is partly because of pion production, but also because of some contribution from the spectators at this high energy. The 80 plastic scintillators may also be used to study two-particle correlations in the azimuthal angle. The degree of equilibration which seems to be observed in single particle inclusive data may be due to the averaging of many collisions. Two-particle correlations[10] may tell us about the degree of equilibration in each collision.[11] In fact in low multiplicity events we have already observed a correlation, probably partly due to kinematics, that is, an anti-correlation due to conservation of momentum, which decreases for high multiplicity events.

The telescope inside the scattering chamber is shown in Fig. 10. It consists of two Si ΔE detectors followed by 7 cm of Ge made up of two pieces, backed by a reject detector. It measures positive pions from 20 to 100 MeV (75 to 200 MeV/c), protons from 40 to 200 MeV, deuterons up to 250 MeV, and tritons up to 300 MeV. The positive pions must be distinguished from the negative pions which are captured when they stop in the E detector. This is done by observing the delayed coincidence of the π^+-μ^+-e^+ decay from the stopped positive pions with a 2.2 μs mean life. Some typical proton energy spectra observed at several angles to the beam are shown in Fig. 11. They are smooth, fairly flat at forward angles, and exponential at backward angles. For heavier fragments the telescope shown in Fig. 12 was used. It is thinner, with a larger solid angle. Some energy spectra obtained with this telescope are shown in Fig. 13. In Fig. 14 the invariant cross sections for the various fragments at 90^{o} in the laboratory are plotted versus momentum. Surprisingly, the data cluster quite closely. A plot which emphasizes the origin of the emitted fragments is a contour graph of the Lorentz invariant cross section as a function of the transverse momentum/nucleon and rapidity, both relativistic invariants, as shown in Fig. 15. Non-relativistically these variables reduce to the velocity transverse and parallel to the beam, respectively, and a single isotropically emitting source would be represented by circular contours centered at the velocity of the source. Relativistically, the contours are not circles, but similar information can be obtained. It is evident in the figure that for the higher transverse momenta the contours are centered between the rapidity of the target and the rapidity of the projectile. Figure 16 is a similar plot for ^{3}He fragments at three different bombarding energies. At the lower bombarding energy, the rapidity of the target and projectile are close together and our data encompasses both. At the higher bombarding energy our data do not extend very far into the intermediate rapidity region. Some results of Nagamiya et al.[12], taken with a magnetic spectrometer are shown in Fig. 17. While the contours at low transverse momentum are centered near the rapidity of the target, it can be seen that they move to the intermediate rapidity region at large transverse momentum. The pion results of both Nagamiya et al.[12] and Nakai et al.[13] are being discussed in a separate contribution.[14]

These contour graphs clearly show from the experiments that there is an apparent source of intermediate rapidity and high transverse momentum nucleons originating from a central region, and that we do not have merely two interpenetrating nucleon gases. Thus there is hope to study, in one short-lived fused subvolume, the effects of high density and excitation.

The basic reaction mechanism of these complicated reactions must be understood theoretically before we can search for any of the predicted exotic effects of high density and temperature nuclear matter. It may well be like searching for a flower in a field of tall grass. However, this background grass must be understood first, and may be interesting in itself. At present about fifteen different groups of people are attempting calculations involving several very different theoretical frameworks.[15] I will report on two of these which are very different. The first is hydrodynamics which is macroscopic and assumes local equilibrium, and the other is the knock-on cascade calculation which is microscopic and assumes only two particle interactions.

Relativistic hydrodynamics is being used by Amsden, Goldhaber, Harlow, and Nix.[16] They consider two fluids with the coupling between them given by the free nucleon-nucleon cross section. In Fig. 18 are their pictures as a function of time for three different impact parameters. At large impact parameter, notice the clean cuts. At the intermediate impact parameter notice the two groups of spectators and the participants in the third time frame. A comparison with our data is shown in Fig. 19. At forward angles the calculations are low. This disagreement is typical of most of the calculations performed so far. The hydrodynamic approach is promising because it naturally includes an equation of state which may eventually be adjusted to fit a more accurate and complete set of data.

A conventional approach is to extend the Monte Carlo knock-on cascade calculations which have long been used for proton-nucleus reactions. The results of Smith and Danos[17] are shown in Fig. 20 together with our data. The agreement is excellent, however this must be taken with caution because the same program fails to fit proton-nucleus data. However it is interesting to look at their resulting distributions in transverse momentum per nucleon and rapidity, the same variables used above for the contour plots. This is shown in Fig. 21 for a head-on collision. They have fit Maxwellians to their calculations and extracted an apparent temperature to describe the widths of the distributions. In this case you see equal widths of the momentum distributions in the transverse and parallel directions, which means that the cascade code has calculated a random distribution of momenta. However at the more peripheral impact parameters the rapidity distribution is broader than the distribution of transverse momentum/nucleon.

The approach which we have taken is called the nuclear fireball model.[18] It involves three concepts: geometry, kinematics, and thermodynamics. The geometry consists of the clean cuts shown in Fig. 2 which separate the participants from the spectators. The geometry also tells us what fraction of the participants comes from the projectile, and therefore by kinematics, the forward velocity of the fireball and the energy in the fireball system. The thermodynamics assumes that this energy in the fireball is thermalized and that the fireball decays as an ideal gas. Actually, if there is enough energy to excite nucleon isobars then these are included by the method used by Hagedorn[19] for nucleon-nucleon collisions. Comparisons of the fireball calculations with our data are shown in Fig. 22. The fit is good considering that there are no adjustable parameters. The calculated properties of the fireball are shown in Table I. The second line with a temperature of 28 MeV can be compared to the much more elaborate cascade calculations of Smith and Danos[17] in Fig. 21, where the width of their distributions was represented by a temperature of 32 MeV. In the first case listed you can see that there appears to be about 60 nucleons with a temperature of about 50 MeV. Thus, this is apparently a piece of nuclear matter at very high temperature. The fireball model has been extended by Myers[20] to include a diffuse surface and the variation of the velocity and temperature across the fireball as shown in Fig. 23. There is increased yield at the lower energies and better agreement with the data.

None of the theories described so far can calculate the emission of high energy particles heavier than nucleons. Our first attempt at this was to describe the composite particles, deuterons, tritons, etc., as coming from the coalescence of nucleons.[21] Therefore their spectra could be obtained from the proton spectrum raised to a certain power. The fits are reasonable as shown in Fig. 24. Later it occurred to two groups[22,23] that the composite particles could be made in equilibrium in the fireball by a method similar to explosive nucleosynthesis. Mekjian's fits[22] in Fig. 25 are also good. This approach is more interesting, because it yields information on the density of the expanding fireball when the equilibrium is frozen out.

It has been proposed[10] that one could obtain the size and lifetime of the fireball from the small angle correlations by an adaptation of the method proposed by Hanbury-Brown and Twiss to measure the size of stellar objects. This method has also been used recently with pions to measure the size and lifetime of the nucleonic fireball.[24] When applied to protons from the nuclear fireball by Koonin[25] the small angle azimuthal correlation calculated is shown in Fig. 26. For protons of the same energy and polar angle there is a repulsion at zero azimuthal angle separation due to Fermi statistics and Coulomb repulsion, and an attraction at slightly larger azimuthal angles due to the nuclear force acting over the size and lifetime of the fireball. This is a difficult experiment, but one which is being planned. However, it may be that the yield of deuterons which has already been measured contains similar information about the small angle correlation of nucleons.[22]

The exciting study of central collisions of relativistic heavy ions has been in progress only two years. The first sets of experimental data have stimulated enormous theoretical interest and several methods are approaching the ability to describe the gross features of the single particle inclusive data. It is not clear yet which method will be most successful, nor is it clear which will be most useful as a framework for searching for the anticipated exotic effects. Experimentally it appears that we have seen high temperature, but not yet, high density nuclear matter. Although most theories predict a factor of 4 to 5 increase in density in the initial interaction, the signature expected in the laboratory for this high density needs more work. Certainly more accurate and more exclusive experimental data are needed on protons, on light fragments, and on low energy pions. In this new field we are rapidly progressing through the grass while the search for the flowers is just beginning.

ACKNOWLEDGMENTS

In all aspects of this work I would like to acknowledge the stimulating collaboration of my colleagues, Jean Gosset, Hans Gutbrod, Jannik Johansen, Chris Lukner, Bill Meyer, Andres Sandoval, Reinhard Stock, and Gary Westfall. In particular I would like to thank Andres Sandoval and Reinhard Stock for suggestions concerning this paper. For permission to quote their calculations, I would like to acknowledge Ray Nix, Kent Smith, Bill Myers, Aram Mekjian, and Steve Koonin. For permission to quote their experimental results, I would like to acknowledge Harry Heckman, Robert Poe, Lee Schroeder, and Shoji Nagamyia. This work was done with support from the U. S. Energy Research and Development Administration, from the Bundesministerium für Forschung and Technologie, W. Germany, and from the Gesellschaft für Schwerionen Forschung, Darmstadt, W. Germany.

REFERENCES

1) J. D. Bowman, W. J. Swiatecki, and C. F. Tsang, LBL report 2908 (1973); W. J. Swiatecki, unpublished report (1976).

2) H. H. Heckman, D. E. Greiner, P. J. Lindstrom, and D. D. Tuttle, "An Atlas of Heavy Ion Fragmentation Topology", LBL report, 1976, unpublished.

3) Third Summer Study on High-Energy Heavy-Ion Physics, Lawrence Berkeley Laboratory, July 12-16, 1976.

4) S. Y. Fung, W. Gorn, G. P. Kiernan, F. F. Liu, J. J. Lu, Y. T. Oh, J. Ozawa, R. T. Poe, C. Van Dalen, L. Schroeder and H. Steiner, unpublished (1977).

5) R. Stock and A. M. Poskanzer, Comments on Nuclear and Particle Physics VII, No. 2, p. 41 (1977).

6) T. D. Lee, Rev. Mod. Phys. 47, 267 (1975).

7) A. B. Migdal, preceding paper, this conference.

8) J. Gosset, H. H. Gutbrod, W. G. Meyer, A. M. Poskanzer, A. Sandoval, R. Stock, and G. D. Westfall, Phys. Rev. C 16, 629 (1977).

9) J. Hüfner and J. Knoll, unpublished (1977).

10) G. J. Kopylov, Phys. Lett. 50B, 472 (1974).

11) S. E. Koonin, unpublished (1977).

12) S. Nagamiya, I. Tanihata, S. R. Schnetzer, W. Bruckner, L. Anderson, G. Shapiro, H. Steiner and O. Chamberlain, unpublished (1977).

13) K. Nakai, J. Chiba, I. Tanihata, S. Nagamiya, H. Bowman, J. Ioannou and J. O. Rasmussen, unpublished (1977).

14) S. Nagamiya, contributed paper, this conference.

15) A. A. Amsden, J. N. Ginocchio, F. H. Harlow, J. R. Nix, M. Danos, E. C. Halbert and R. K. Smith, Jr., Phys. Rev. Letters 19, 1055 (1977).

16) A. A. Amsden, A. E. Goldhaber, F. H. Harlow, and J. R. Nix, unpublished (1977).

17) R. K. Smith and M. Danos, unpublished (1977).

18) G. D. Westfall, J. Gosset, P. J. Johansen, A. M. Poskanzer, W. G. Meyer, H. H. Gutbrod, A. Sandoval, and R. Stock, Phys. Rev. Letters 37, 1202 (1976).

19) R. Hagedorn and J. Ranft, Nuovo Cimento 6, 300 (1968).

20) W. D. Myers, unpublished (1977).

21) H. H. Gutbrod, A. Sandoval, P. J. Johansen, A. M. Poskanzer, J. Gosset, W. G. Meyer, G. D. Westfall, and R. Stock, Phys. Rev. Letters 37, 667 (1976).

22) A. Mekjian, Phys. Rev. Letters 38, 640 (1977), and unpublished (1977).

23) J. Bond, P. J. Johansen, S. E. Koonin, and S. Garpman, unpublished (1977).

24) A. T. Laasanen, C. Ezell, L. J. Gutay, W. N. Schreiner, P. Schübelin, L. von Lindern, and F. Turkot, Phys. Rev. Letters 38, 1 (1977).

25) S. E. Koonin, unpublished (1977).

Table I. Fireball parameters at the impact parameter with the maximum weight (b_{MW}).

PROJECTILE	TARGET	b_{MW} (fm)	ε (MeV/n)	β	N	τ (MeV)
400 MeV/n Ne	U	4.8	74	0.27	64	47
250 MeV/n Ne	U	4.8	44	0.22	64	28
400 MeV/n ^{4}He	U	4.7	51	0.17	25	34

XBL 776-9102

FIGURE CAPTIONS

Fig. 1. A view of the Bevalac showing the SuperHILAC and the Bevatron.

Fig. 2. A schematic representation of a relativistic heavy ion collision showing the projectile fragment, the target spectator, and in the center, the participating nucleons which will be referred to as the nuclear fireball.

Fig. 3. The interaction of a 1.8 GeV/nucleon Ar ion in a nuclear emulsion.[2]

Fig. 4. The interaction of a 1.8 GeV/nucleon Ar ion with a lead target in a streamer chamber.[4]

Fig. 5. Charged particle multiplicity distributions deduced from streamer chamber data.[4]

Fig. 6. Sketch of the binding energy per nucleon versus nuclear matter density in units of the equilibrium density.[5]

Fig. 7. (Top) a schematic of the spherical scattering chamber. (Bottom) The array of plastic scintillators as seen looking down the beam line.

Fig. 8. Three events obtained with the 80-counter array of scintillators for 400 MeV/nucl. ^{40}Ar on Ca.

Fig. 9. The average multiplicity plotted versus the multiplicity expected from the clean cut assumption.[9] The symbols, □, 0, and ◊ refer to U, Ca, and Al targets, respectively. The dashed line is drawn through the 1.05 GeV/nucleon data.

Fig. 10. The Si-Ge telescope used for measuring the spectra of pions, protons, deuterons, and tritons.

Fig. 11. Double differential cross sections obtained for protons from 400 MeV/nucleon Ar ions on U. This is the most recent set of data and is still preliminary.

Fig. 12. The Si-Ge telescope used for the heavier fragments.[8] The boron nitride had the shape of a window frame. The telescope had an active area of 20 cm^2.

Fig. 13. Double differential cross sections for the heavier fragments obtained[8] from 400 MeV/nucleon ^{20}Ne ions on U.

Fig. 14. Invariant cross sections[8] at 90° in the laboratory from 400 MeV/nucleon ^{20}Ne ions on U.

Fig. 15. Contour plots[8] of invariant cross sections versus transverse momentum per nucleon and rapidity from 400 MeV/nucleon ^{20}Ne ions on U. Every third curve which shows the data points is labelled by the logarithm of the invariant cross section in mb/sr MeV^2. Rapidity is defined as $y = 1/2 \ln[(E + p_{11})/(E - p_{11})]$.

Fig. 16. Contour plots for ^3He fragments at three different bombarding energies[8] of ^{20}Ne on U.

Fig. 17. Contour plot for protons from Nagamyia et al.[12]

Fig. 18. Relativistic hydrodynamic calculations[16] for 250 MeV/nucleon ^{20}Ne ions on U.

Fig. 19. Relativistic hydrodynamic calculations[16] (histograms) compared to experimental data. Actually, added to the proton data are the d and t data, plus twice the ^3He and ^4He data, at the same velocity.

Fig. 20. Cascade calculations[17] (histograms) compared to experimental proton data.

Fig. 21. Distributions of transverse momentum per nucleon and rapidity obtained from the cascade calculations.[17]

Fig. 22. The fireball calculations[8] (solid lines) compared to experimental data. The proton spectra from a uranium target are at the angles 30°, 60°, 90°, 120°, and 150°, except that in the middle graph the 150° data are missing.

Fig. 23. The fire streak model.[20] The shading is proportional to temperature and the dashed contours represent evaporation from the hot region.

Fig. 24. The coalescence calculations[21] (solid lines) compared to experimental data for ^{20}Ne on U.

Fig. 25. The thermodynamic calculations[22] (solid lines) compared to experimental data for 400 MeV/nucleon ^{20}Ne on U.

Fig. 26. The small-angle azimuthal correlation function calculated for protons of 150 MeV at $\theta = 30°$ for various values of the fireball lifetime.[25]

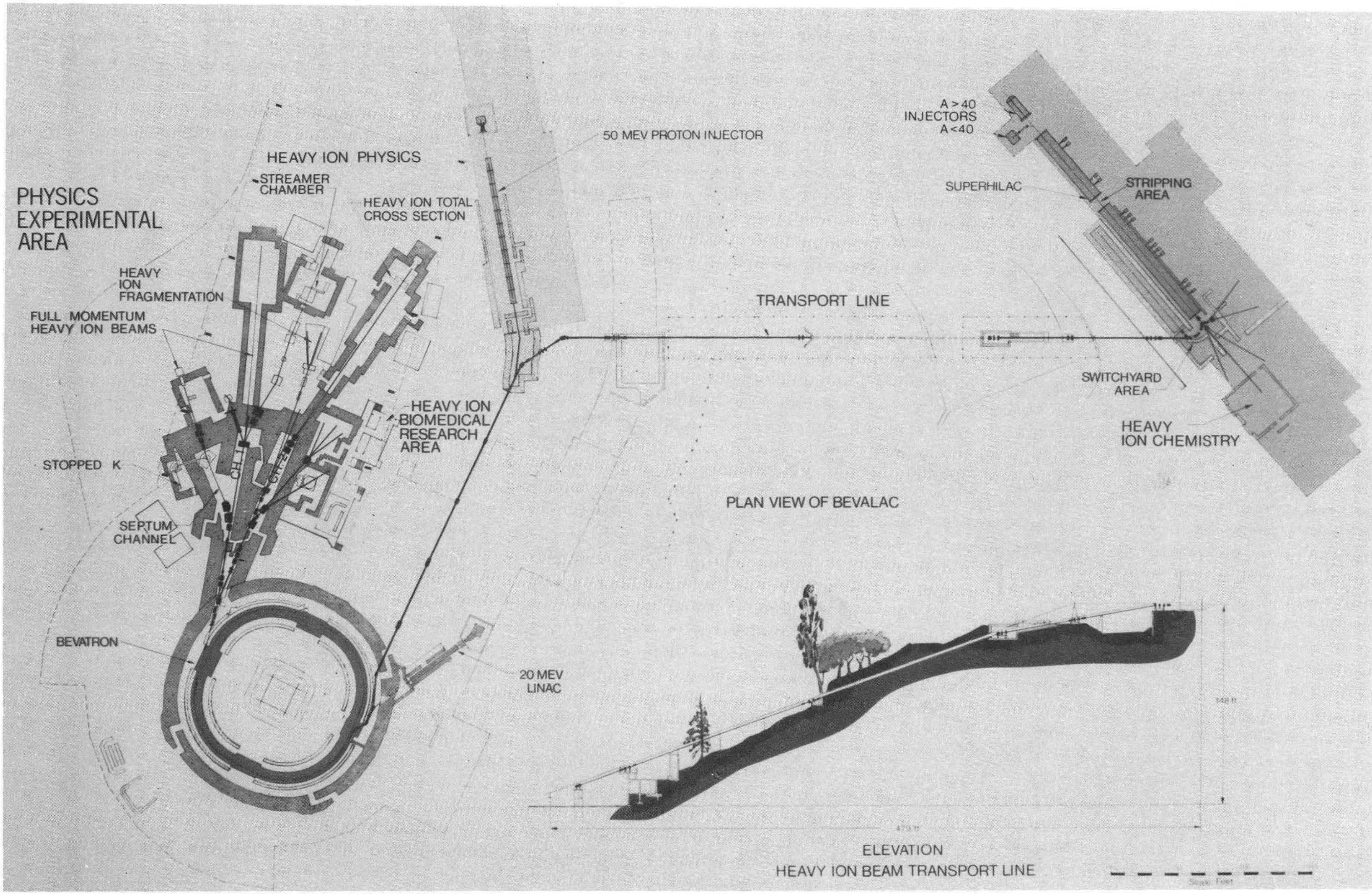

XBB 7511-7911

Fig. 1

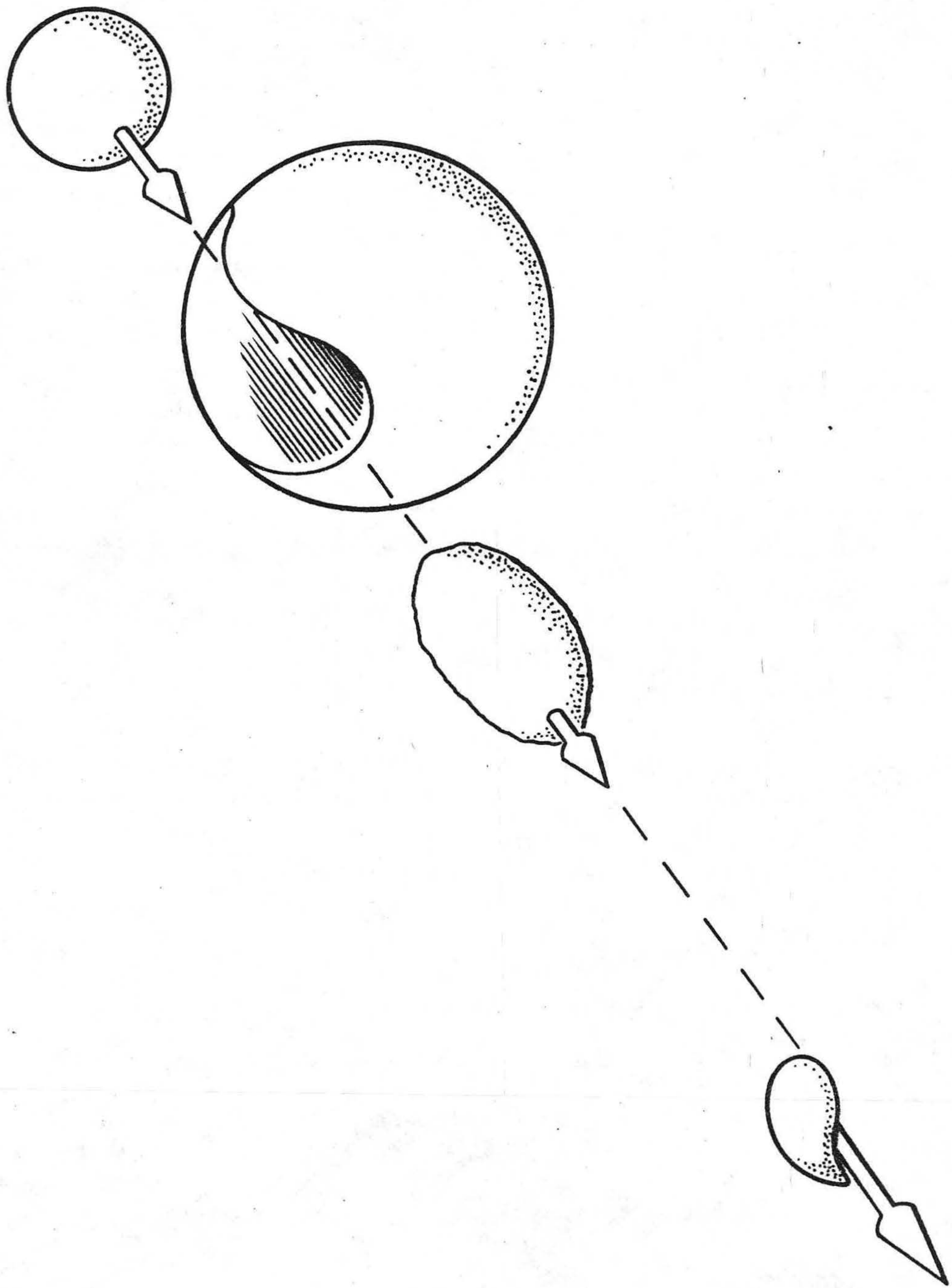

XBL 7610-4265

Fig. 2

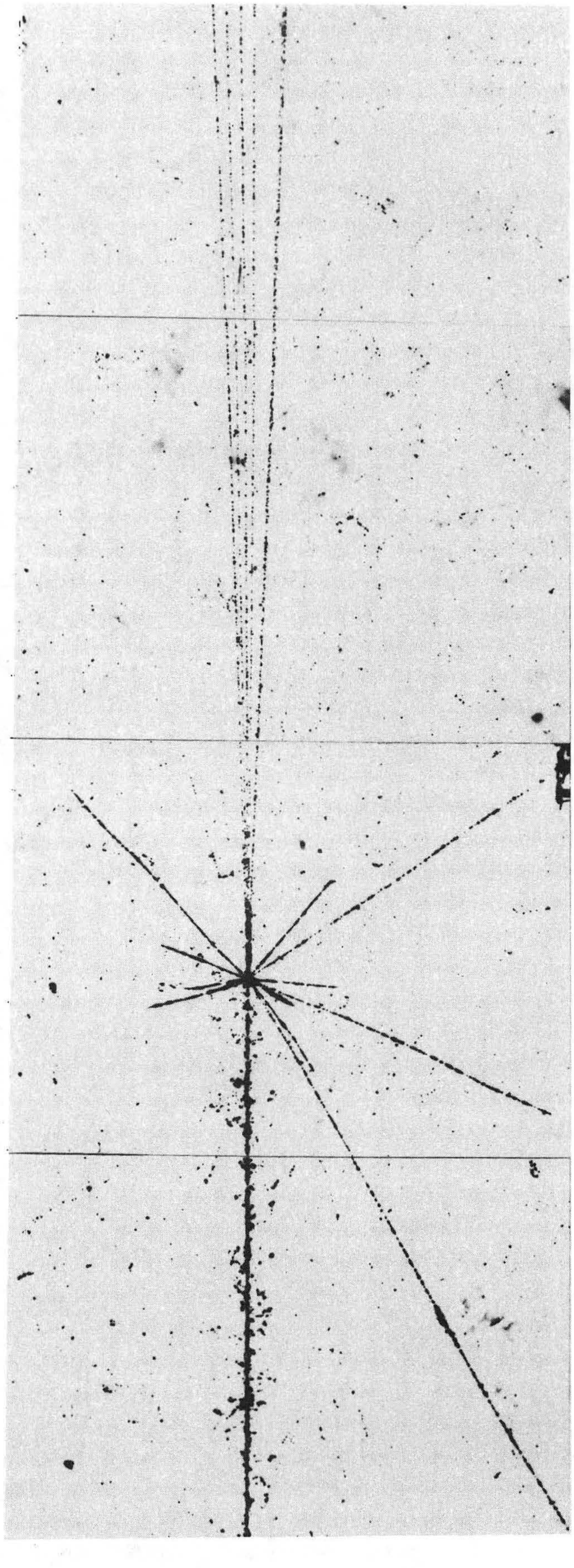

XBB 771-30

Fig. 3

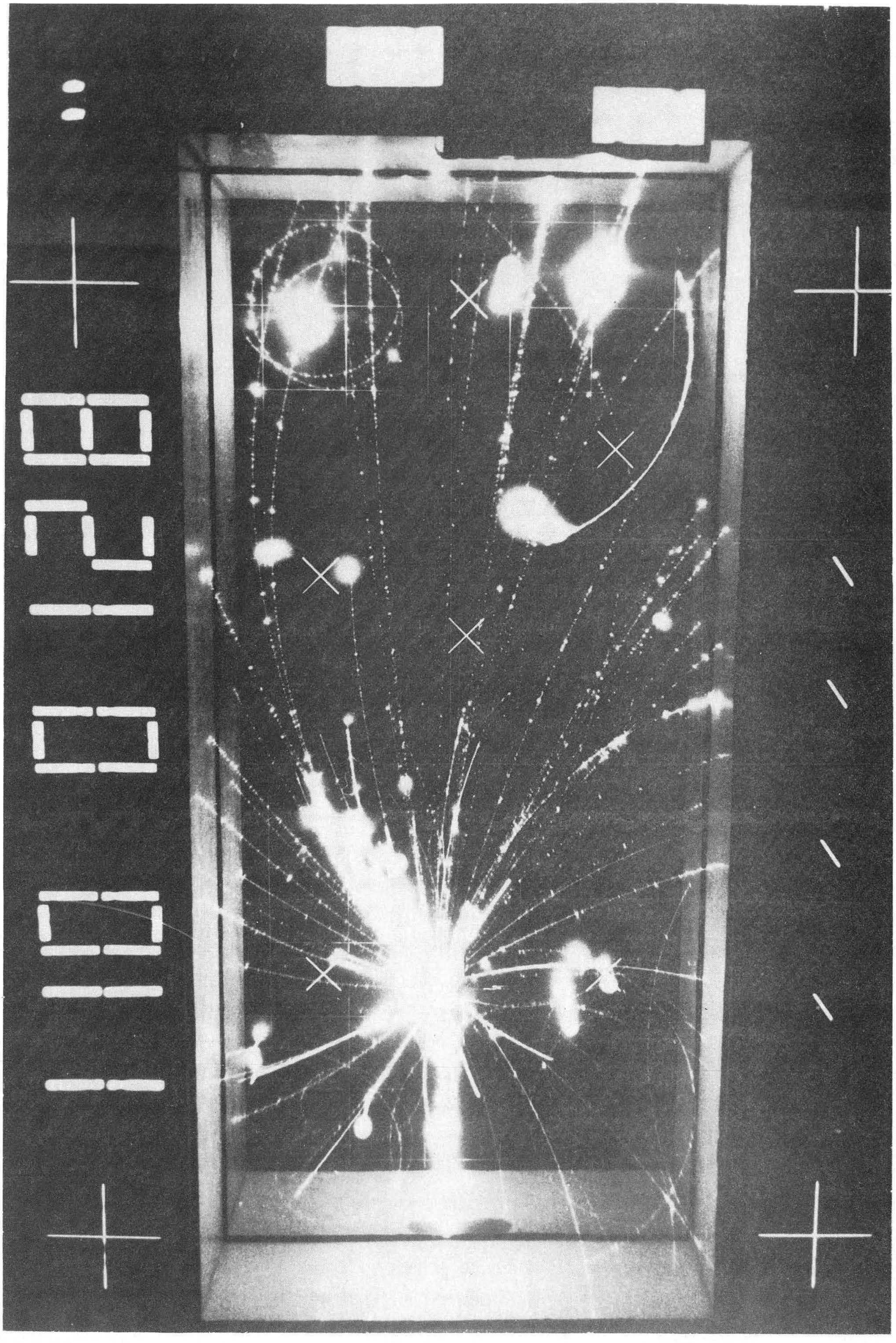

XBB 7511-8444

Fig. 4

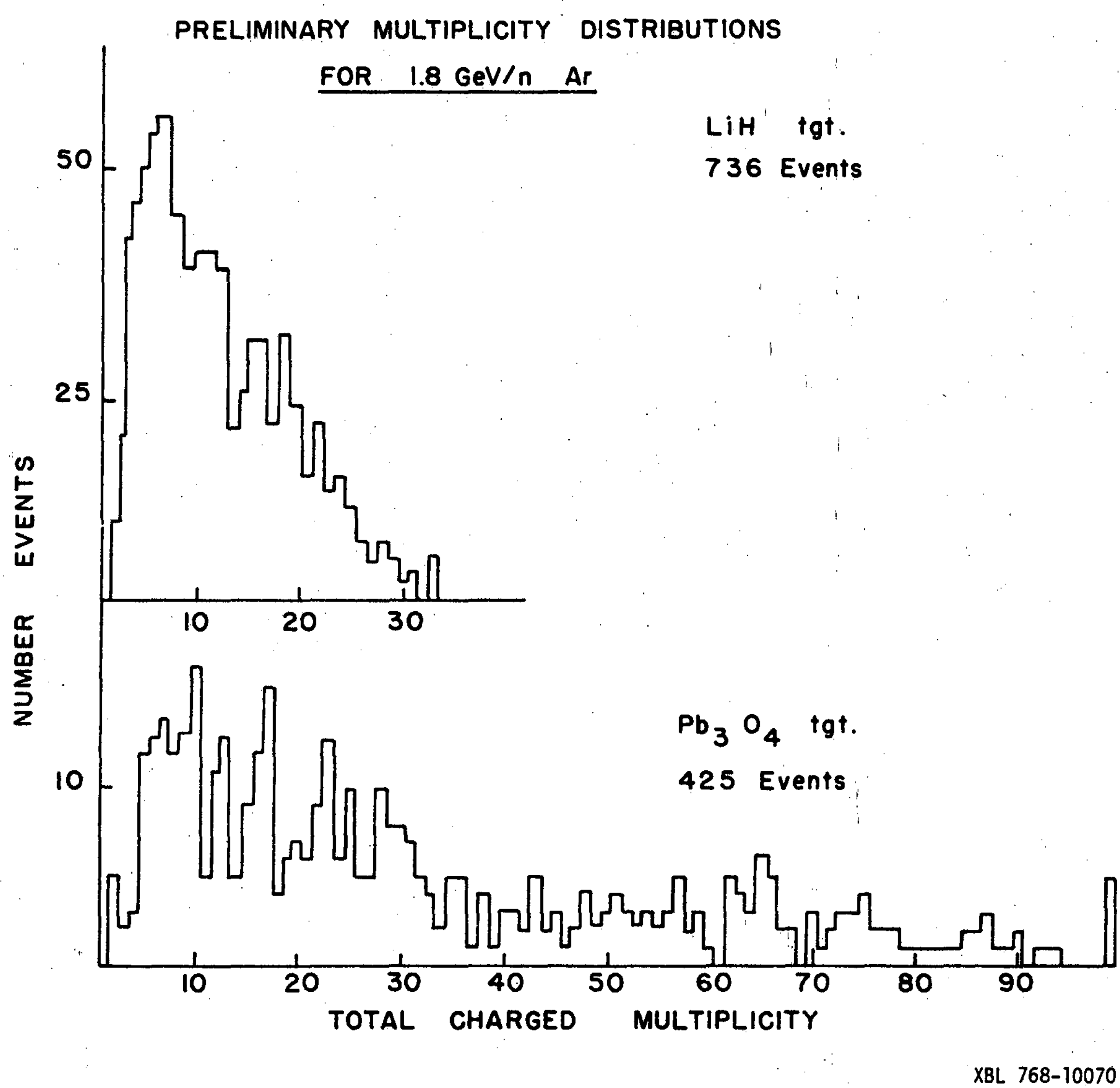
PRELIMINARY MULTIPLICITY DISTRIBUTIONS
FOR 1.8 GeV/n Ar
LiH tgt.
736 Events
50
25
10
20
30
NUMBER EVENTS
Pb3 O4 tgt.
425 Events
10
10
20
30
40
50
60
70
80
90
TOTAL CHARGED MULTIPLICITY
XBL 768-10070

Fig. 5

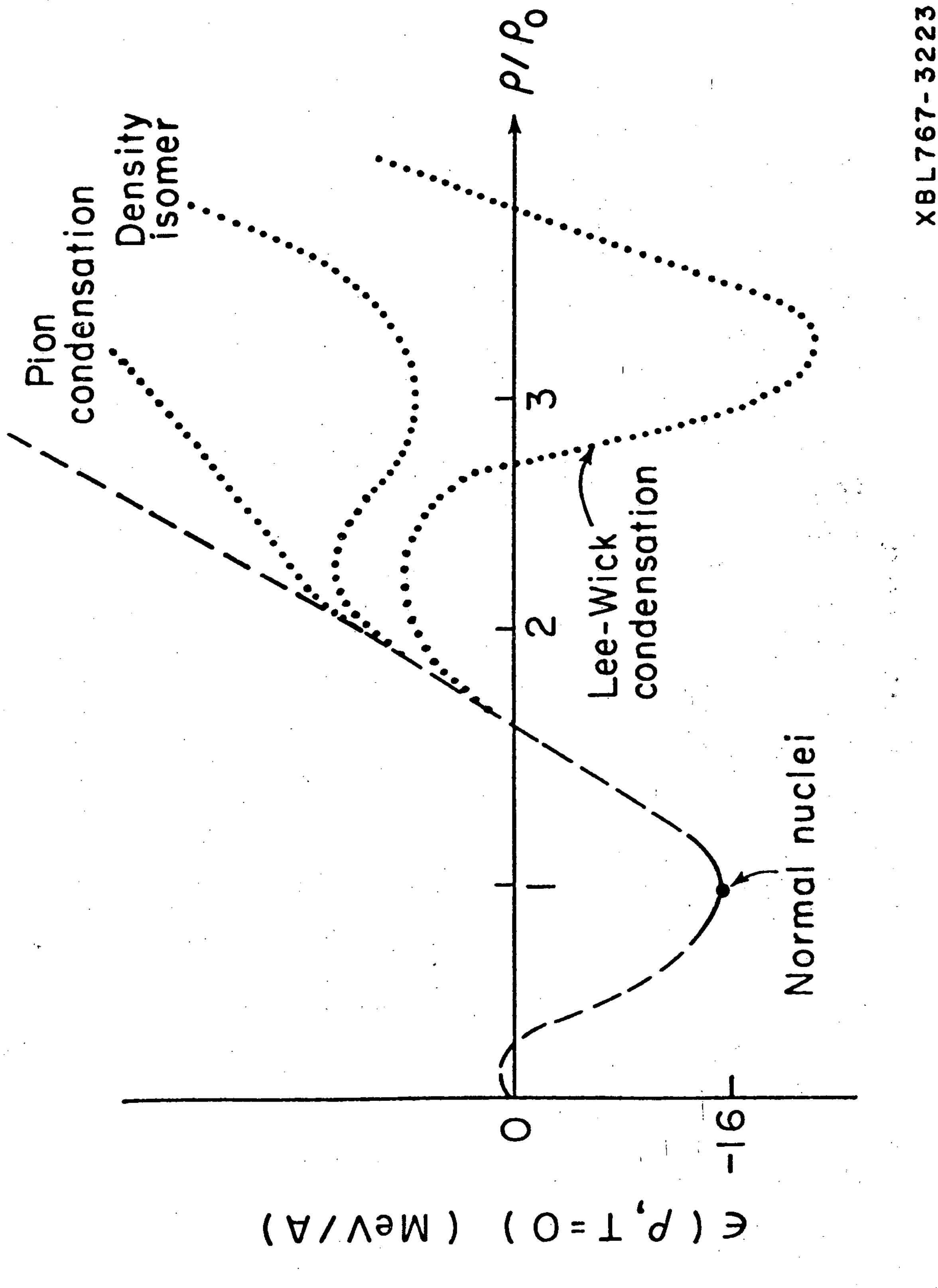
ρ/ρ₀
Pion condensation
Density isomer
Lee-Wick condensation
Normal nuclei
0
-16
1
2
3
ε (ρ, T = 0) (MeV/A)
XBL767-3223

Fig. 6

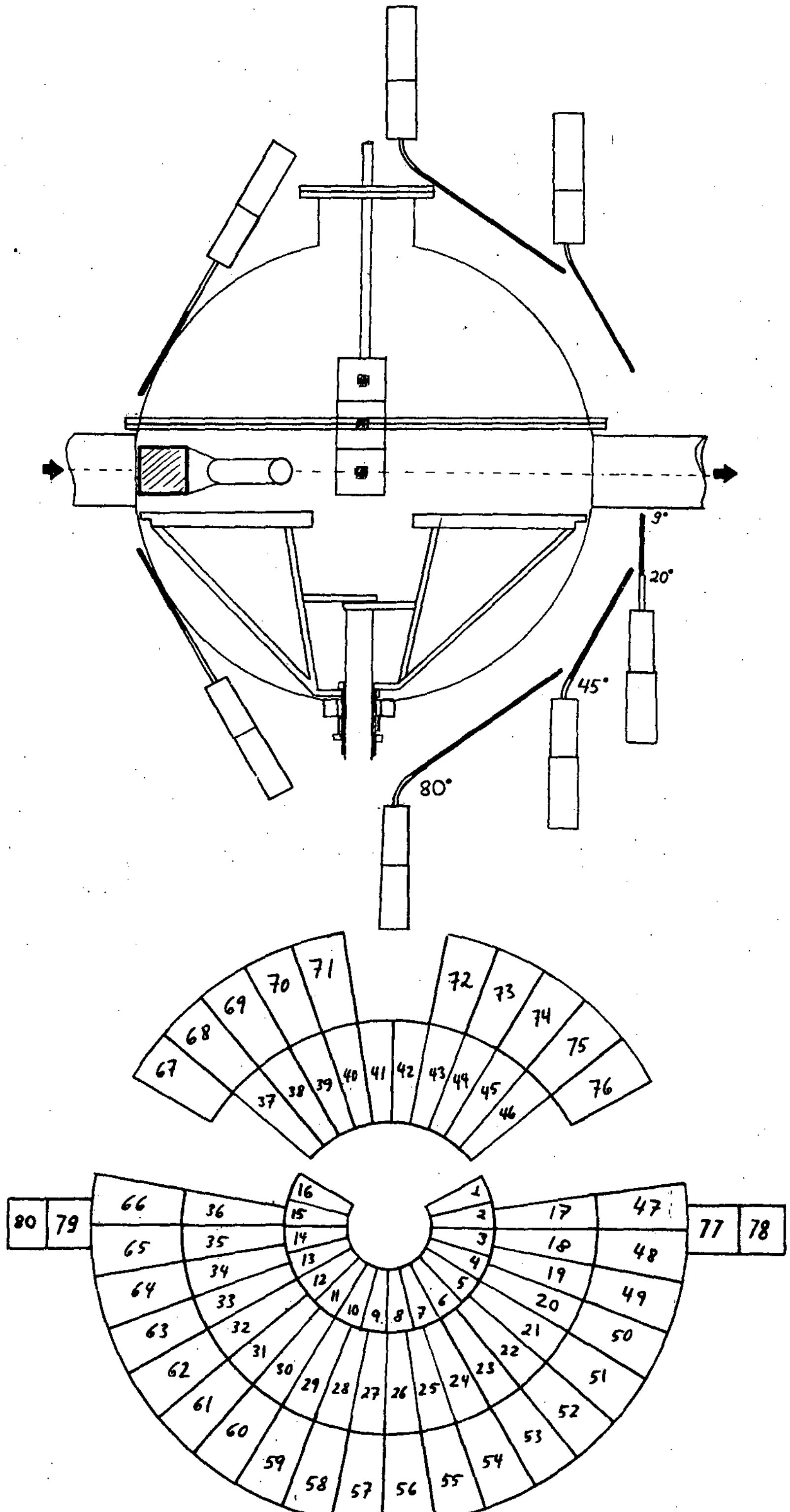

XBL 776-9100

Fig. 7

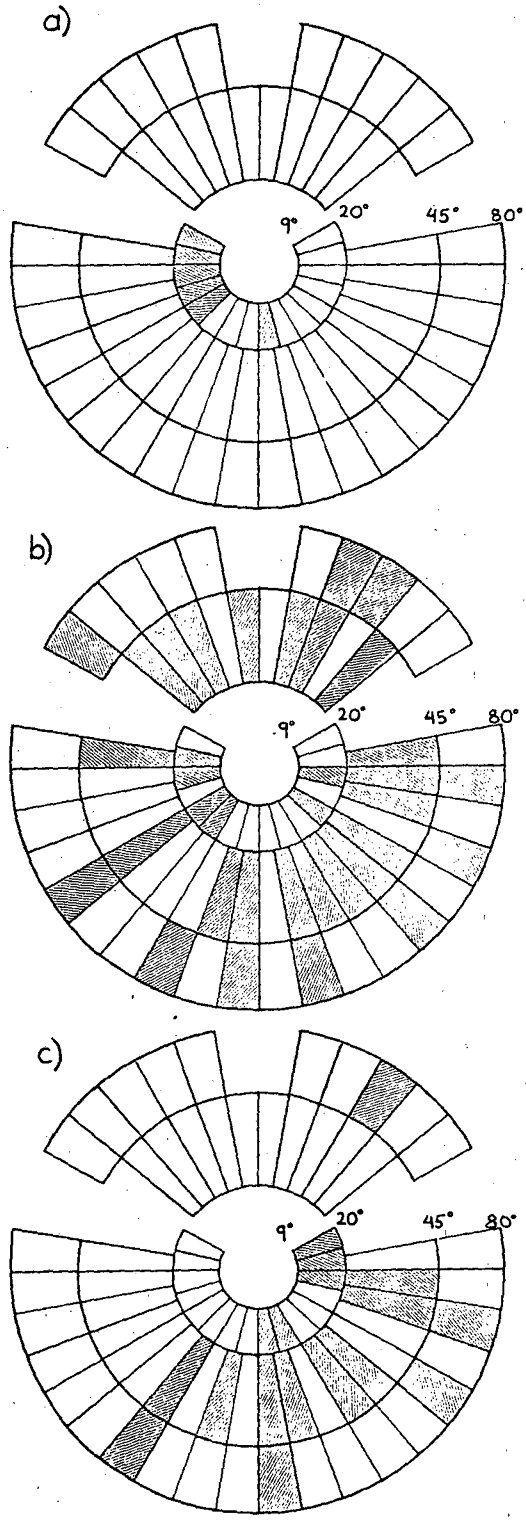

XBL 778-2731

Fig. 8

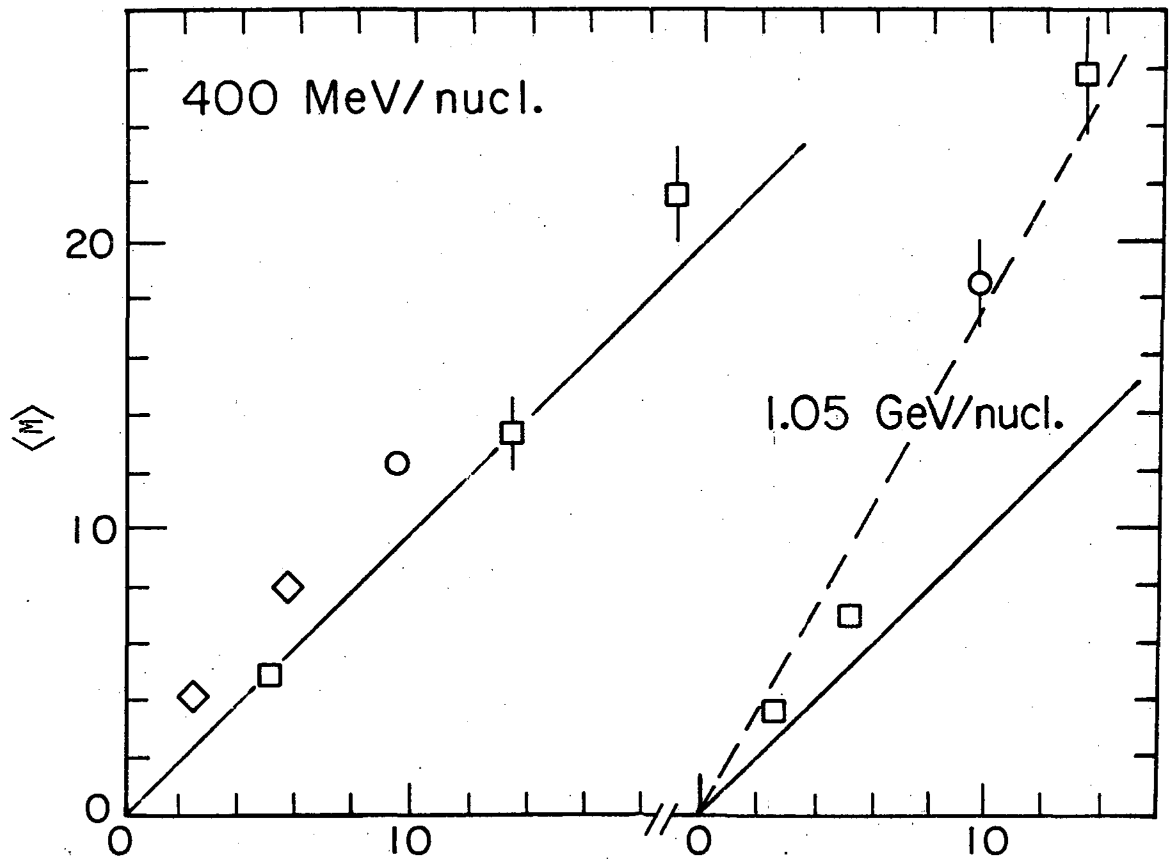

$$R = \frac{\pi r_0^{\,2}\ (Z_t A_p^{-2/3} + Z_p A_t^{\,2/3})}{\pi r_0^{\,2}\ (A_p^{1/3} + A_t^{1/3})^2}$$

XBL 778-2734

Fig. 9

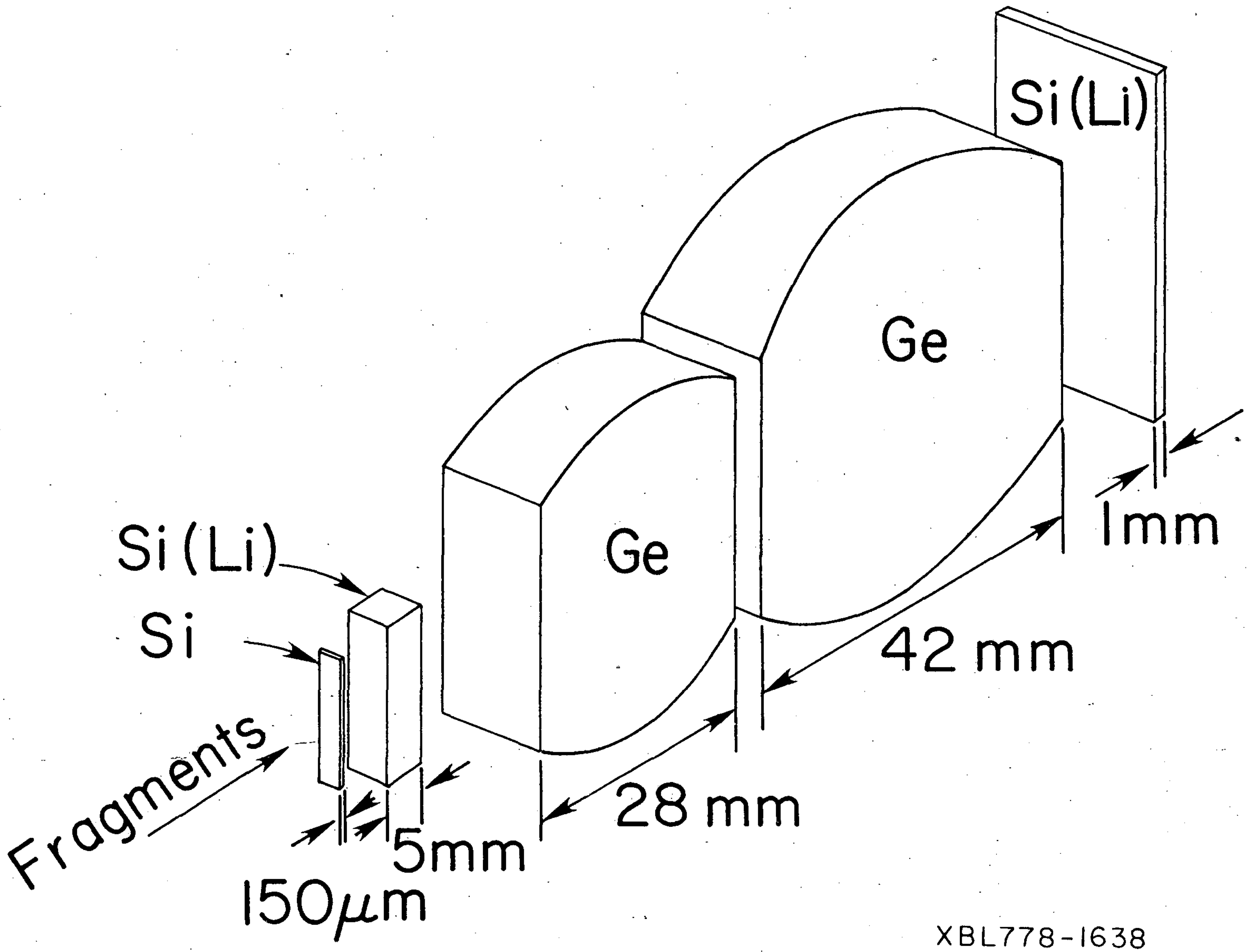
Si(Li)
Ge
Ge
1mm
42 mm
28 mm
Si (Li)
Si
Fragments
5mm
150μm
XBL778-1638

Fig. 10

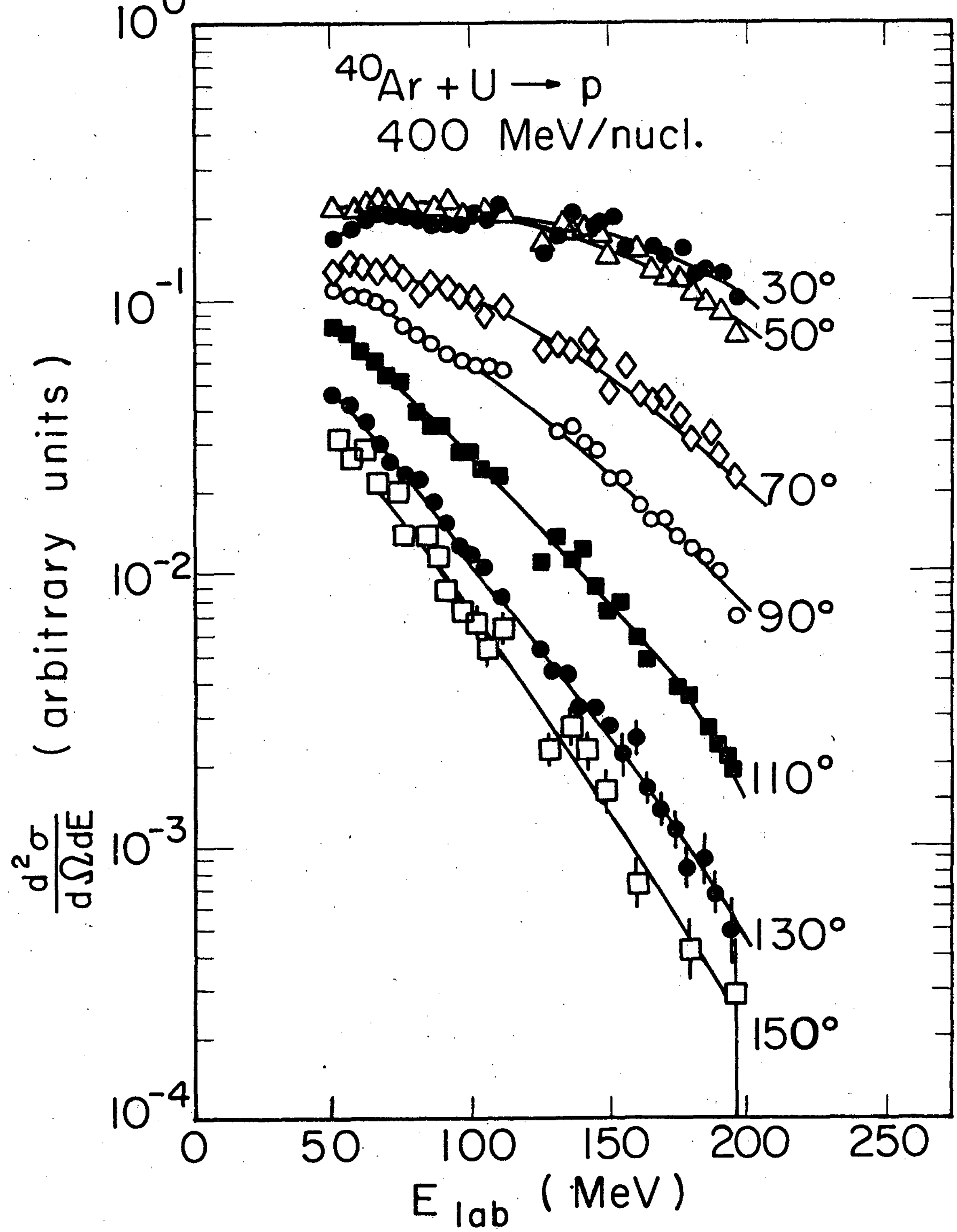

XBL 778-2735

Fig. 11

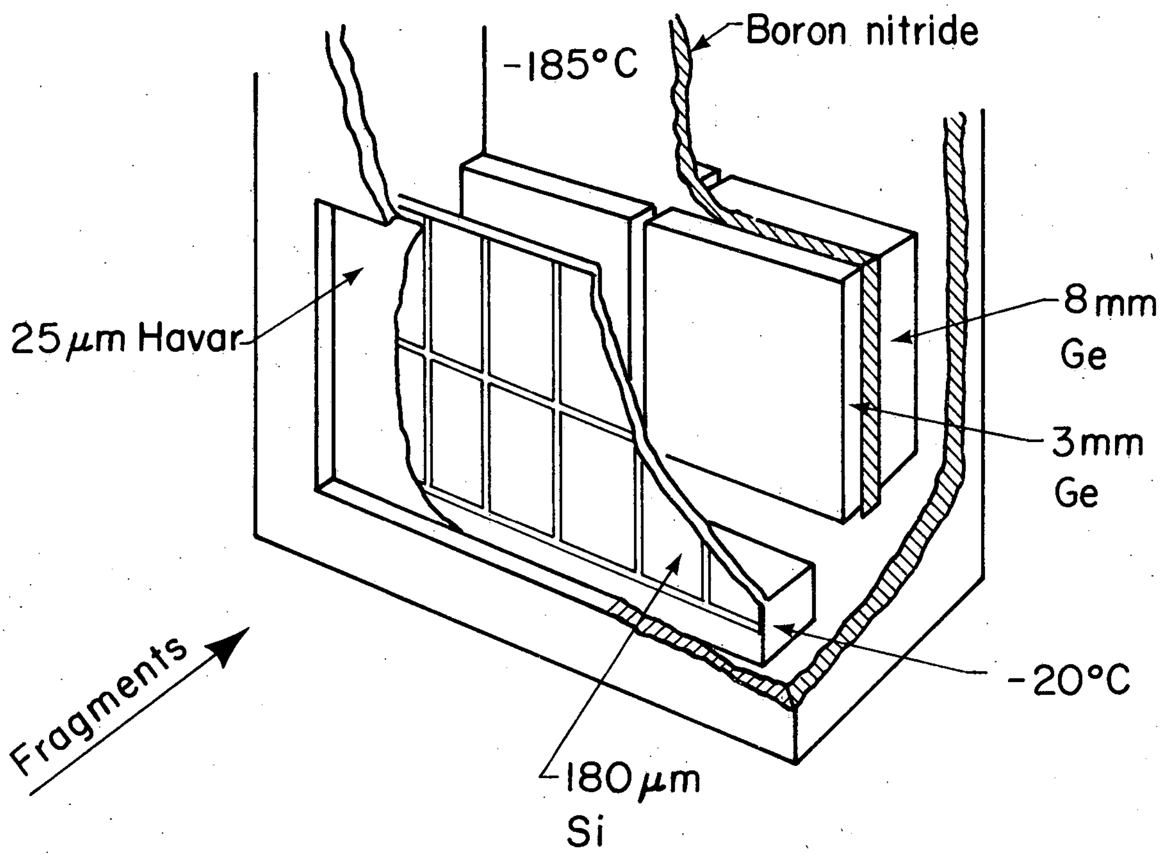

Boron nitride
-185°C
25 μm Havar
8 mm
Ge
3 mm
Ge
Fragments
-20°C
180 μm
Si
XBL 773-545

Fig. 12

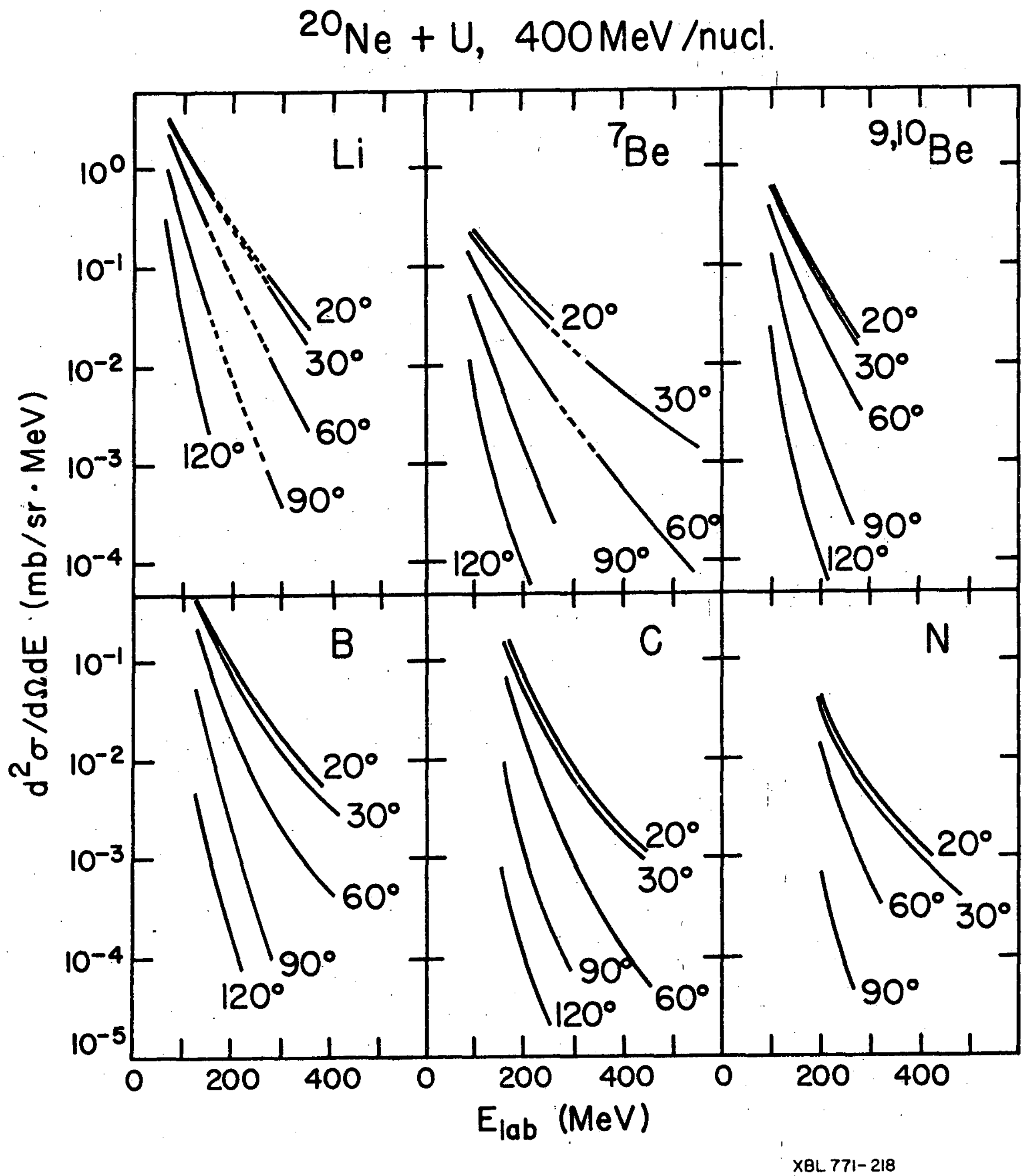
20Ne + U, 400 MeV/nucl.
Li
7Be
9,10Be
B
C
N
20°
30°
60°
90°
120°
d2σ/dΩdE (mb/sr · MeV)
Elab (MeV)
0
200
400
XBL 771-218

Fig. 13

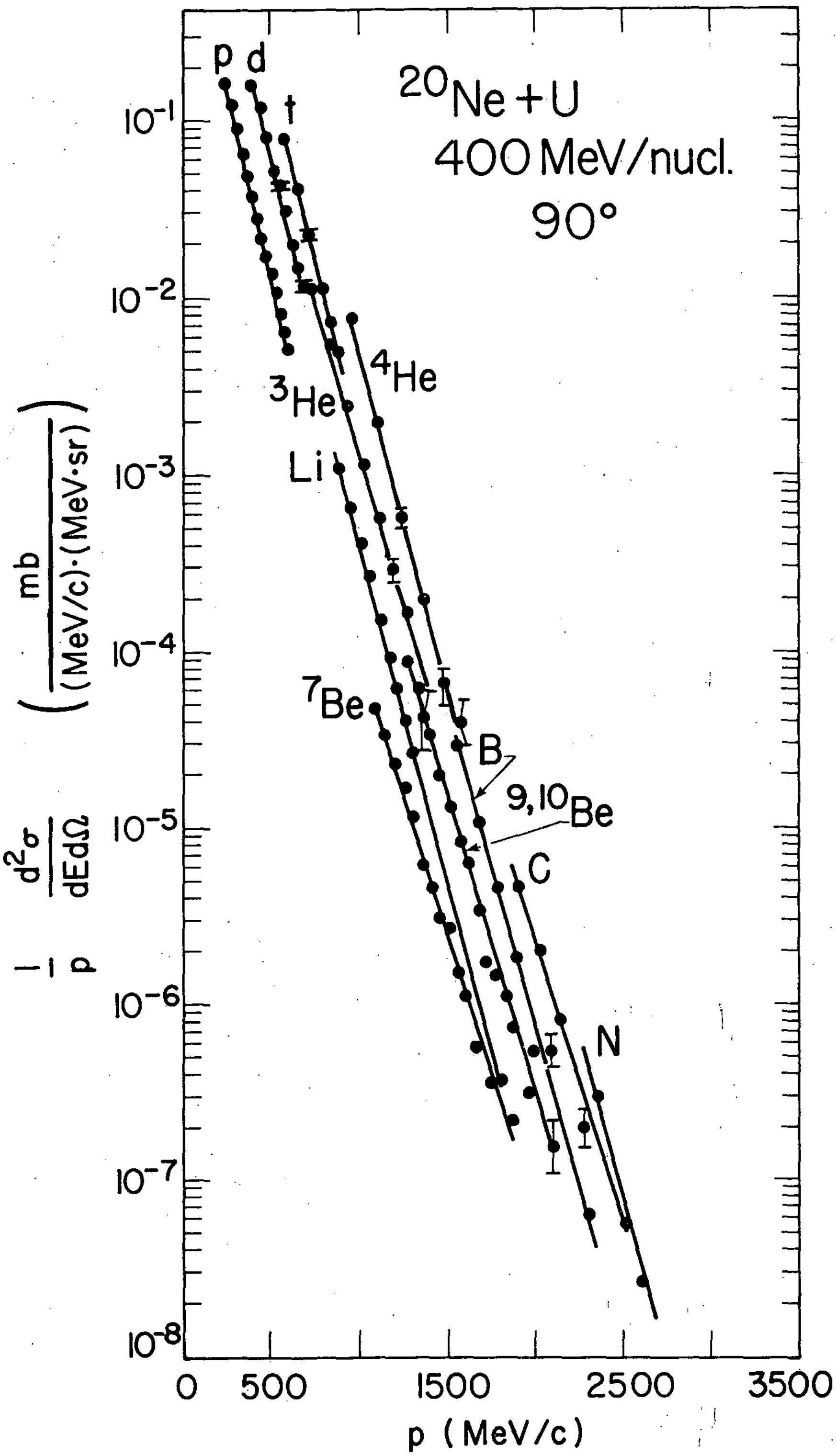

XBL 774-893

Fig. 14

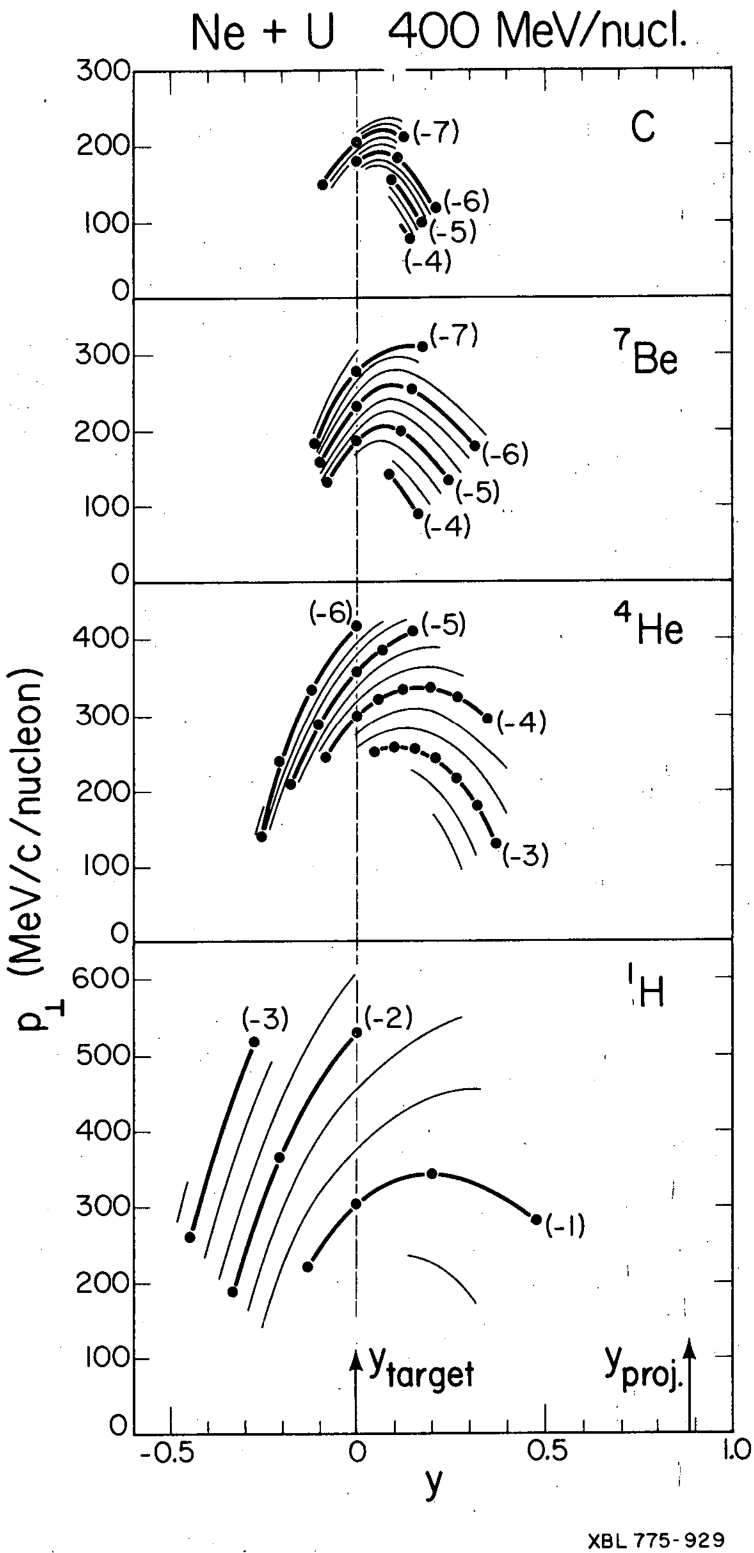

Ne + U 400 MeV/nucl.
C
(-7)
(-6)
(-5)
(-4)
7Be
(-7)
(-6)
(-5)
(-4)
4He
(-6)
(-5)
(-4)
(-3)
1H
(-3)
(-2)
(-1)
p⊥ (MeV/c/nucleon)
y
ytarget
yproj.
-0.5
0
0.5
1.0
XBL 775-929

Fig. 15

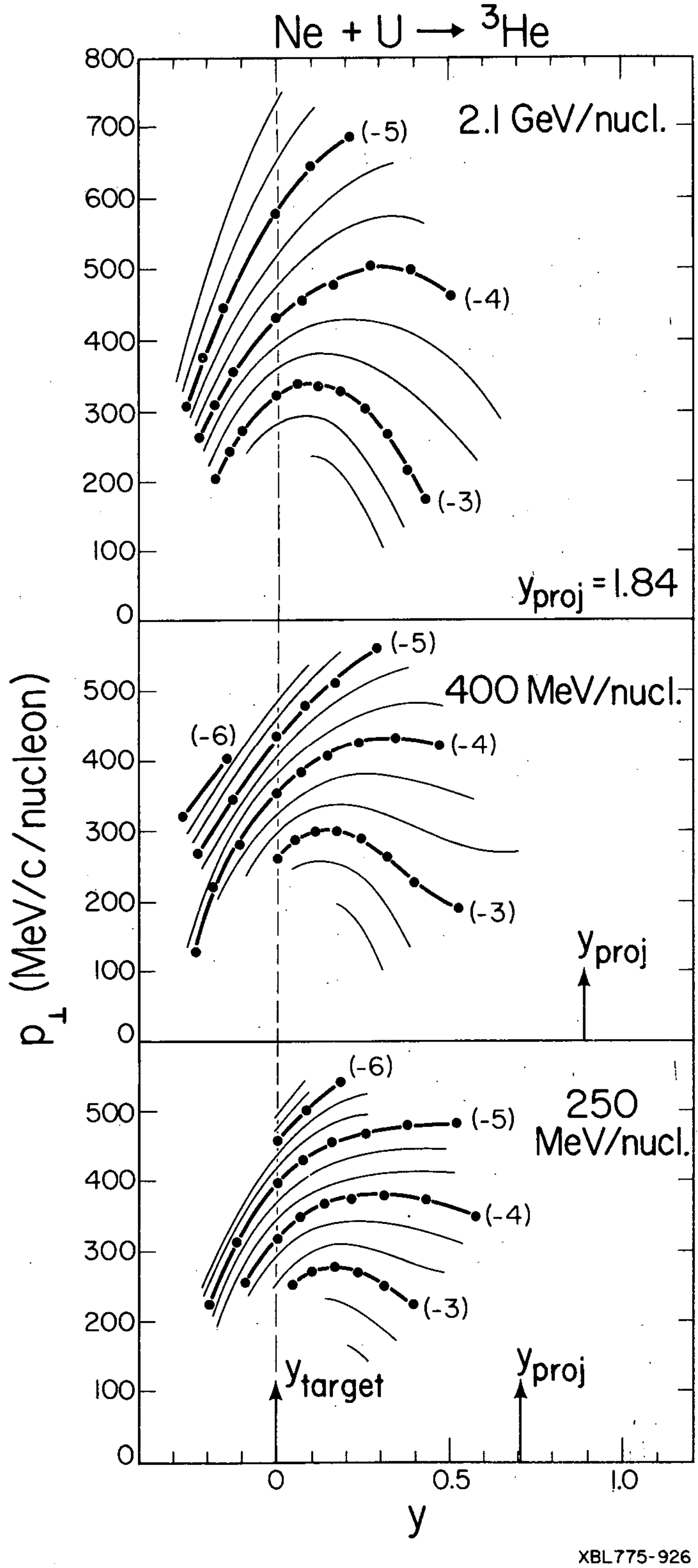

Ne + U → ³He
2.1 GeV/nucl.
y_{proj} = 1.84
400 MeV/nucl.
y_{proj}
250 MeV/nucl.
y_{target}
y_{proj}
(-3)
(-4)
(-5)
(-6)
$p_\perp$ (MeV/c/nucleon)
y
0
0.5
1.0
0
100
200
300
400
500
600
700
800
XBL775-926

Fig. 16

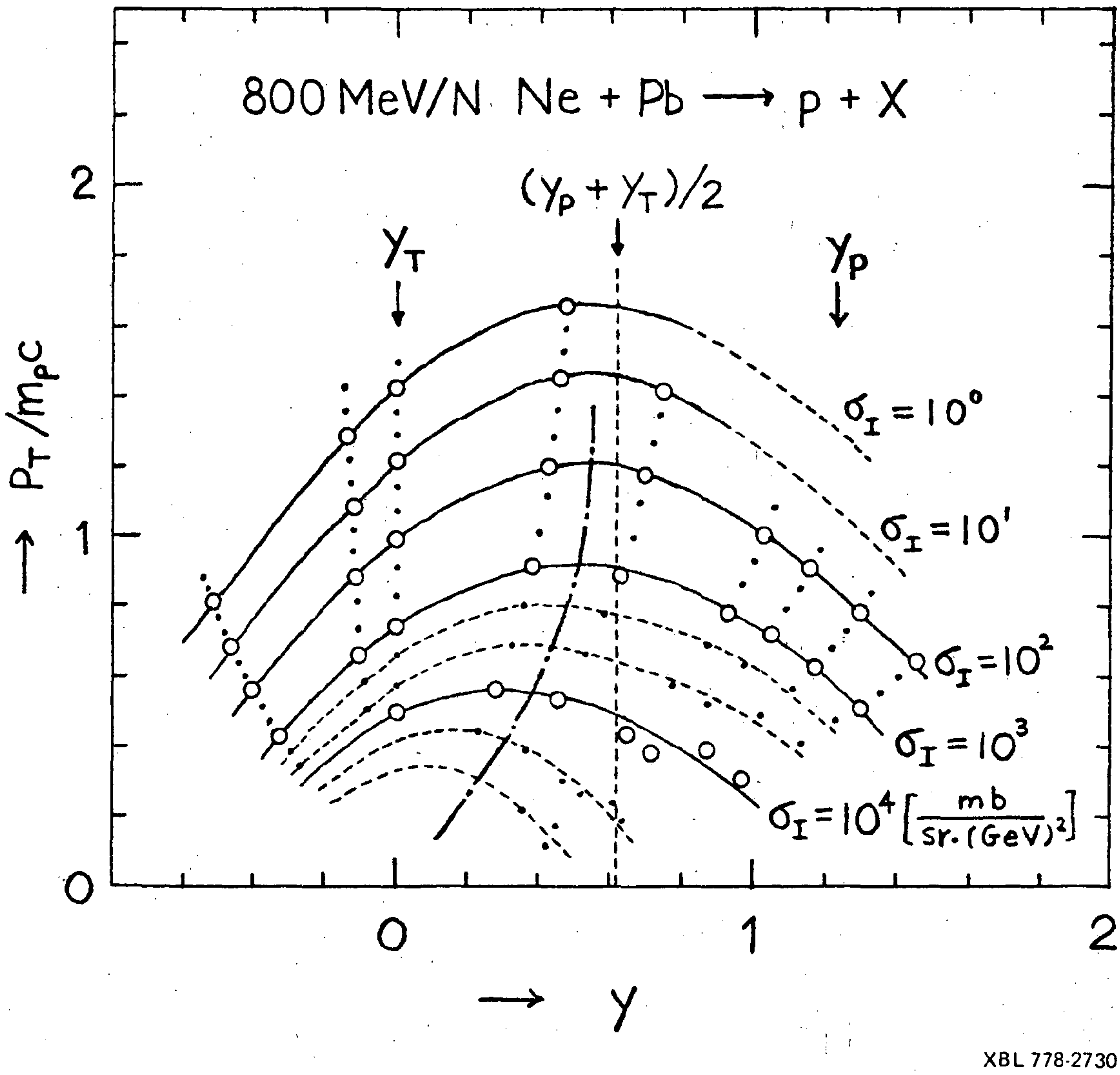
800 MeV/N Ne + Pb ⟶ p + X
$(y_P + y_T)/2$
y_T
y_P
$\sigma_I = 10^0$
$\sigma_I = 10^1$
$\sigma_I = 10^2$
$\sigma_I = 10^3$
$\sigma_I = 10^4 \left[\frac{mb}{sr\cdot(GeV)^2}\right]$
→ P_T/m_pc
→ y
0
1
2
XBL 778-2730

Fig. 17

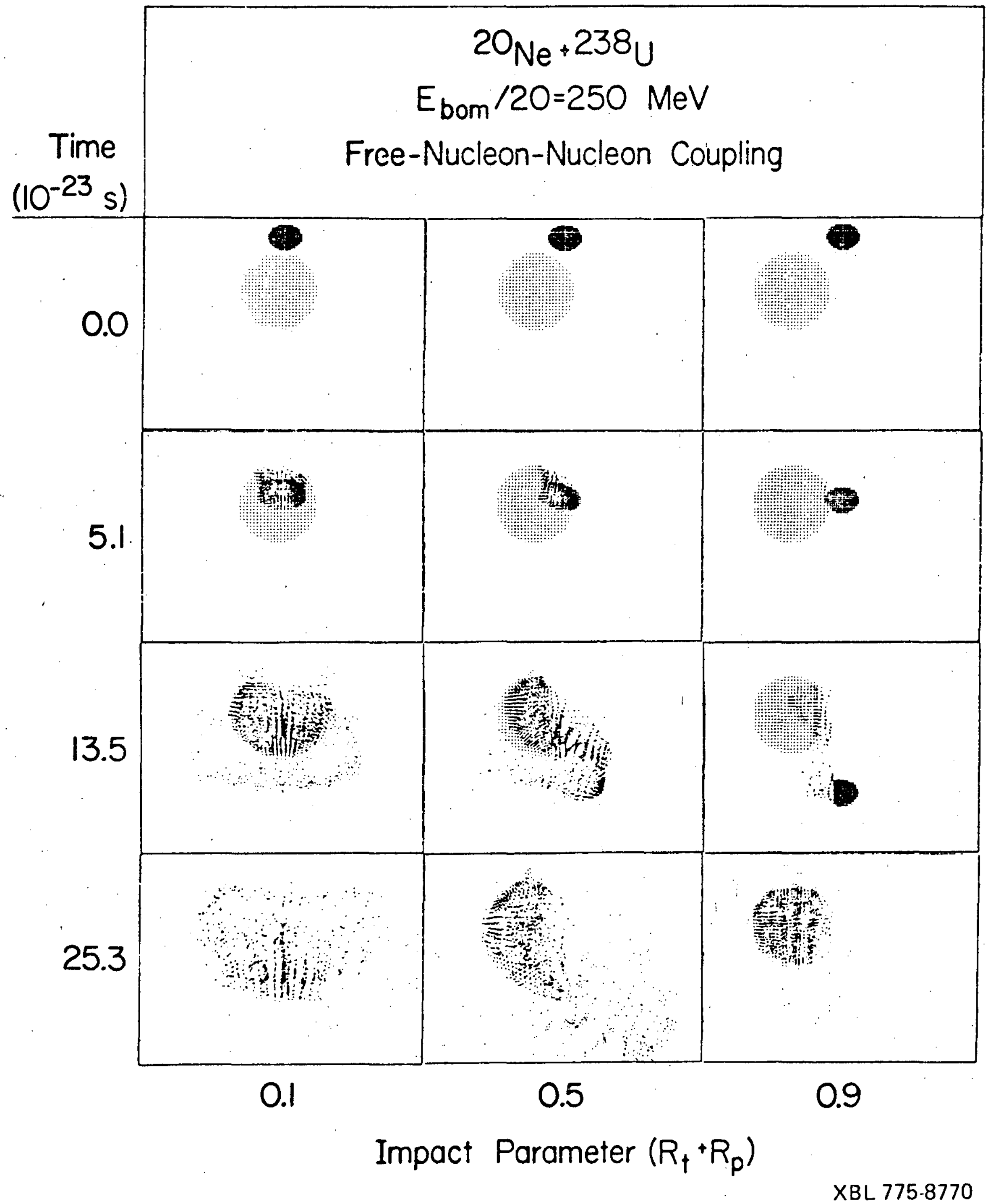
$^{20}Ne + ^{238}U$
$E_{bom}/20 = 250$ MeV
Free-Nucleon-Nucleon Coupling
Time (10^{-23} s)
0.0
5.1
13.5
25.3
0.1
0.5
0.9
Impact Parameter ($R_t + R_p$)
XBL 775-8770

Fig. 18

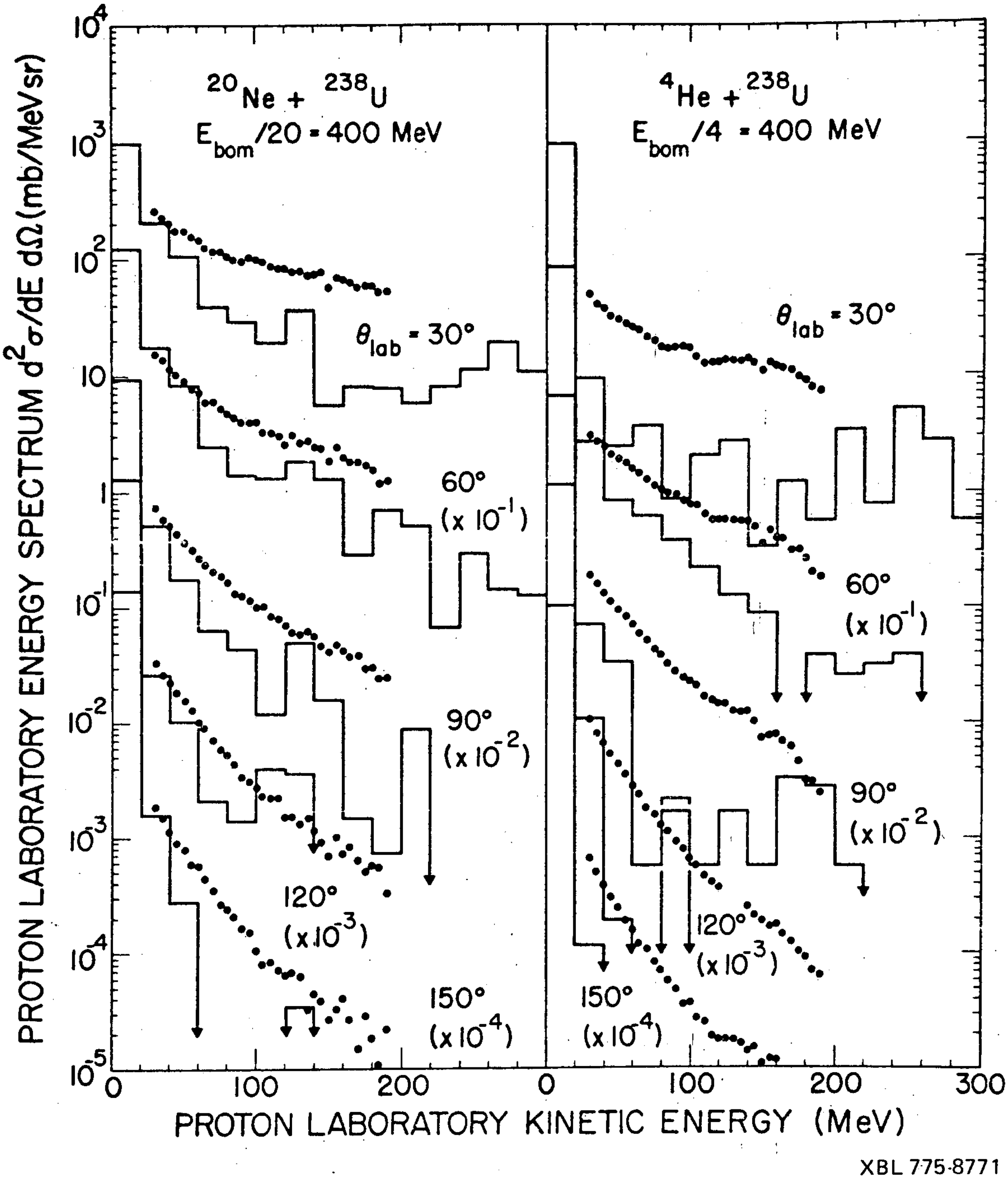

$^{20}Ne + ^{238}U$
$E_{bom}/20 = 400$ MeV
$^{4}He + ^{238}U$
$E_{bom}/4 = 400$ MeV
$\theta_{lab} = 30°$
60° (x 10⁻¹)
90° (x 10⁻²)
120° (x 10⁻³)
150° (x 10⁻⁴)
PROTON LABORATORY ENERGY SPECTRUM $d^2\sigma/dE\,d\Omega$ (mb/MeV sr)
PROTON LABORATORY KINETIC ENERGY (MeV)
XBL 775-8771

Fig. 19

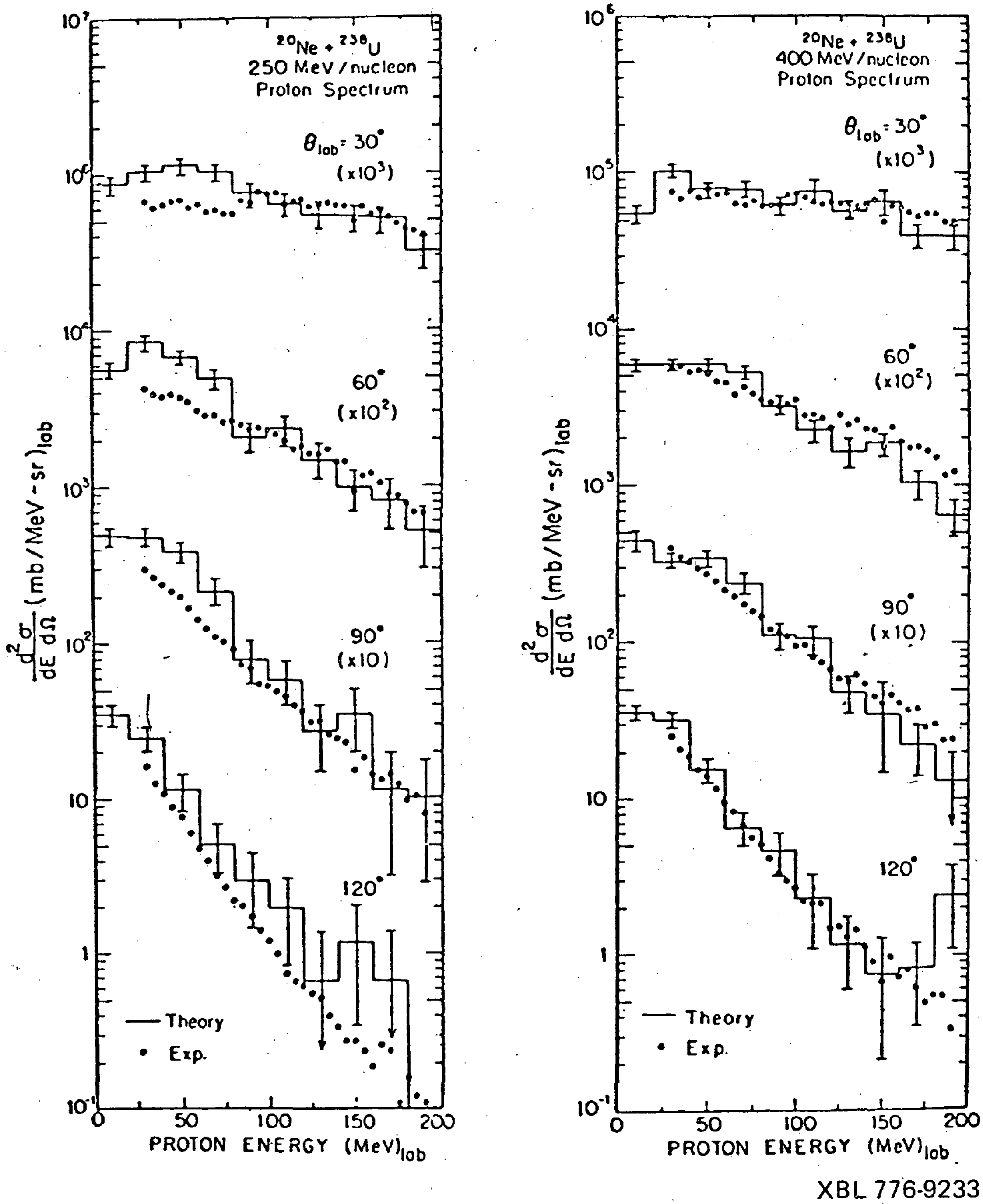

^{20}Ne + ^{238}U
250 MeV/nucleon
Proton Spectrum
θ_{lab} = 30°
(x10^3)
60°
(x10^2)
90°
(x10)
120°
Theory
Exp.
$\frac{d^2\sigma}{dE\,d\Omega}$ (mb/MeV-sr)$_{lab}$
PROTON ENERGY (MeV)$_{lab}$
^{20}Ne + ^{238}U
400 MeV/nucleon
Proton Spectrum
θ_{lab} = 30°
(x10^3)
60°
(x10^2)
90°
(x10)
120°
Theory
Exp.
PROTON ENERGY (MeV)$_{lab}$
XBL 776-9233

Fig. 20

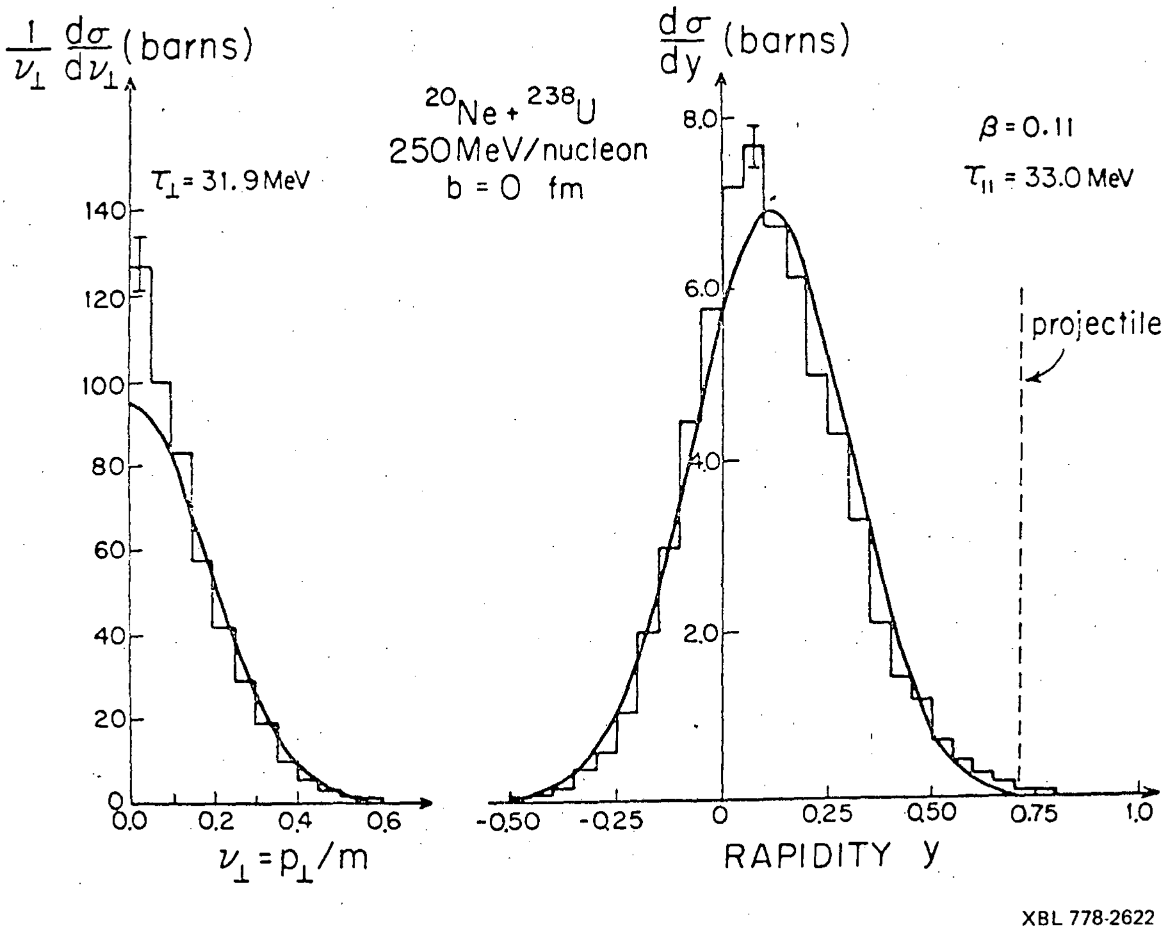

$\frac{1}{\nu_\perp}\frac{d\sigma}{d\nu_\perp}$ (barns)
$\tau_\perp$ = 31.9 MeV
140
120
100
80
60
40
20
0
0.0
0.2
0.4
0.6
$\nu_\perp = p_\perp/m$
^{20}Ne + ^{238}U
250 MeV/nucleon
b = 0 fm
$\frac{d\sigma}{dy}$ (barns)
8.0
6.0
4.0
2.0
β = 0.11
$\tau_\parallel$ = 33.0 MeV
projectile
-0.50
-0.25
0
0.25
0.50
0.75
1.0
RAPIDITY y
XBL 778-2622

Fig. 21

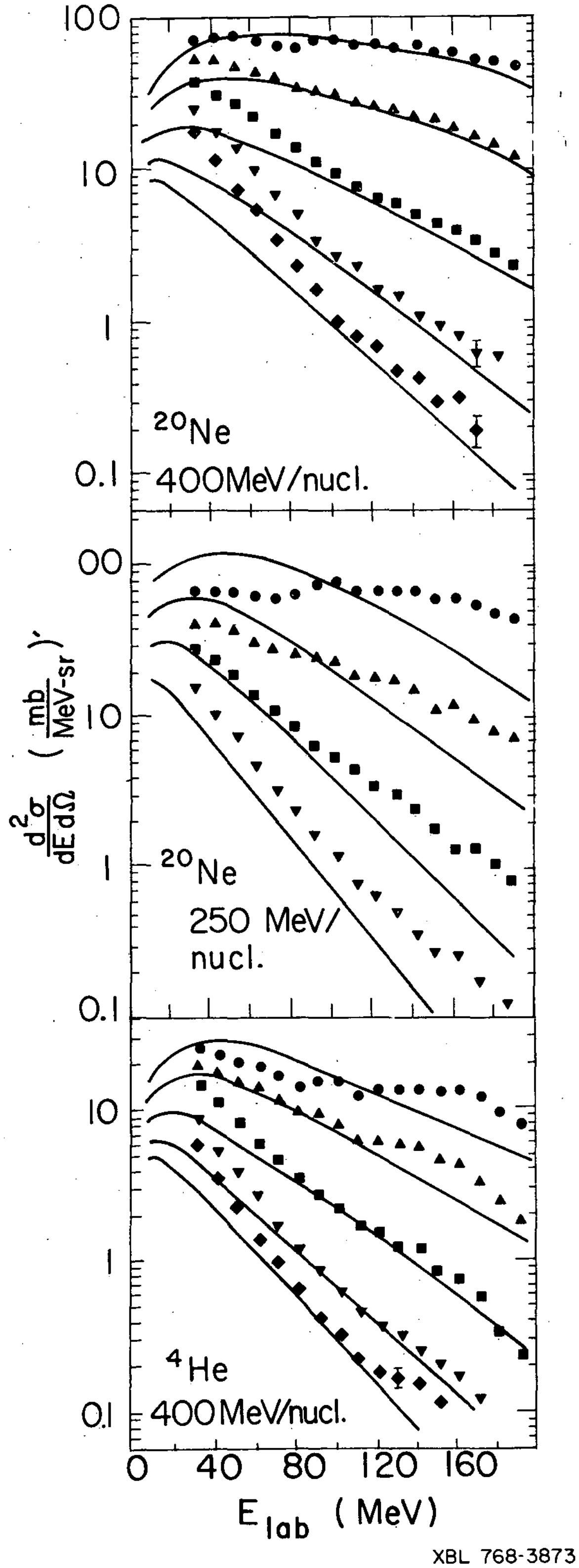
100
10
1
0.1
^{20}Ne
400MeV/nucl.
00
10
1
0.1
$\frac{d^2\sigma}{dE\,d\Omega}$ $\left(\frac{mb}{MeV\text{-}sr}\right)$
^{20}Ne
250 MeV/
nucl.
10
1
0.1
^{4}He
400MeV/nucl.
0 40 80 120 160
E_{lab} (MeV)
XBL 768-3873

Fig. 22

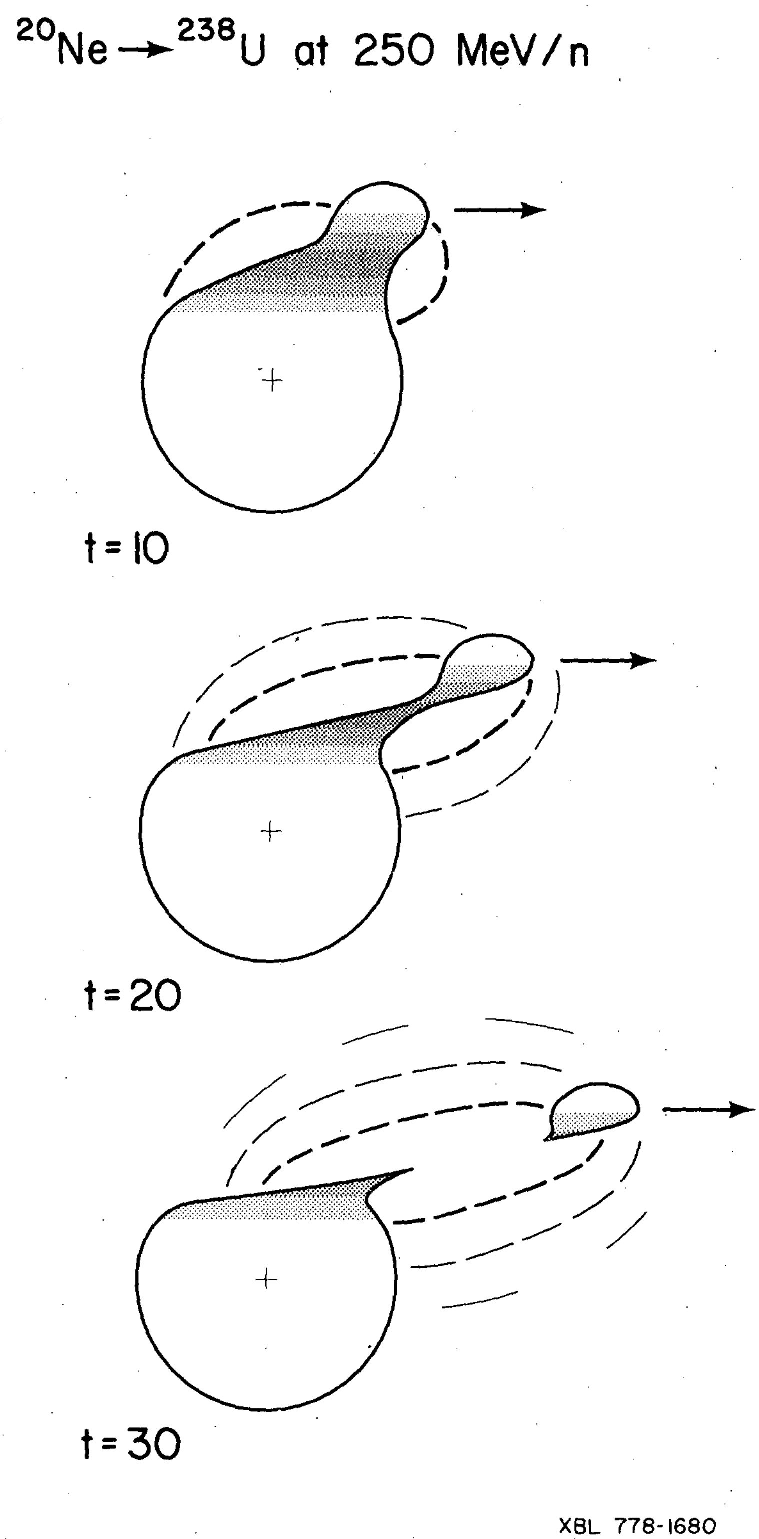

Fig. 23

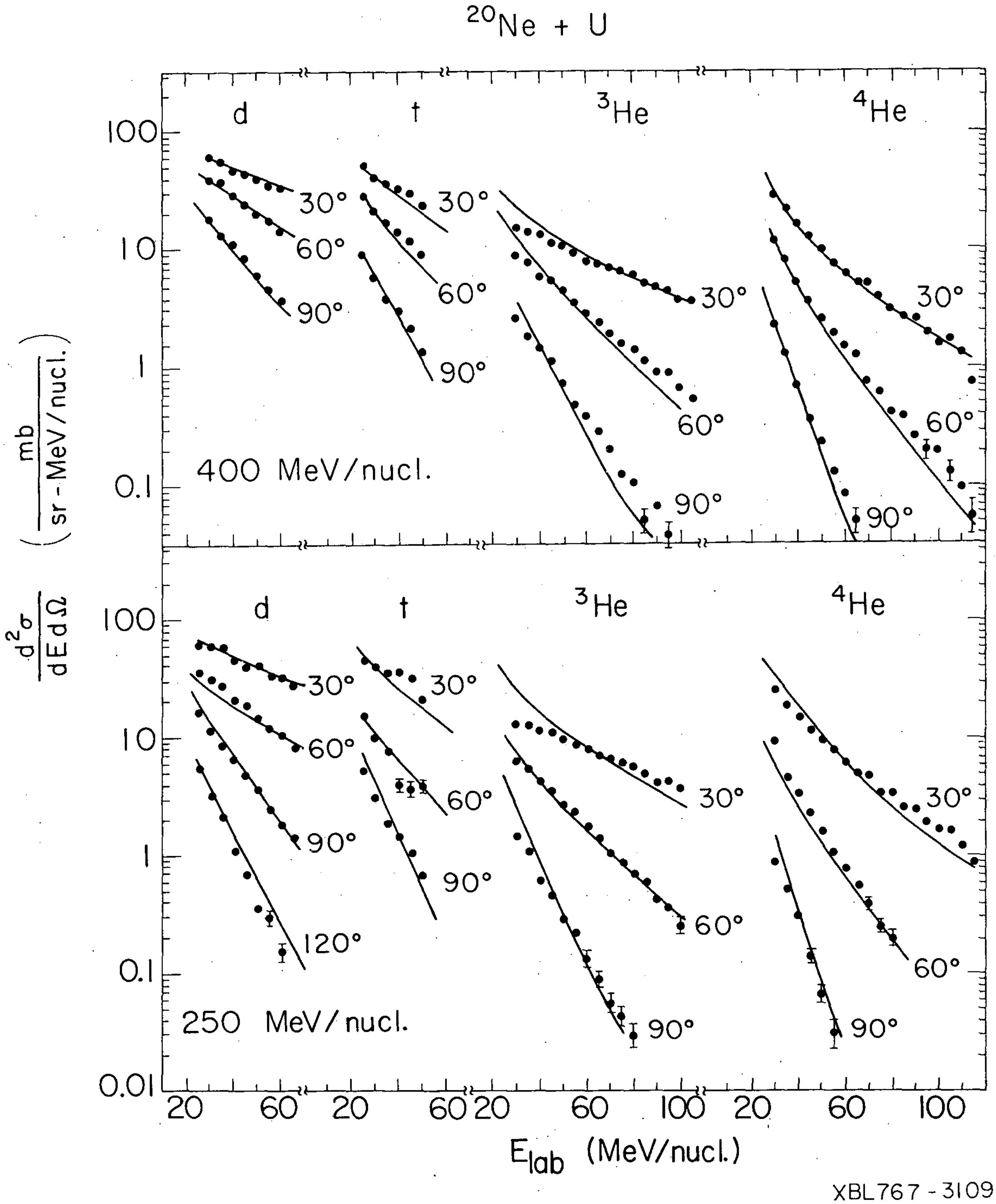

$^{20}Ne + U$
d
t
^{3}He
^{4}He
30°
60°
90°
120°
400 MeV/nucl.
250 MeV/nucl.
100
10
1
0.1
0.01
20
60
100
$\frac{d^2\sigma}{dE\,d\Omega}$ $\left(\frac{mb}{sr\text{-}MeV/nucl.}\right)$
E_{lab} (MeV/nucl.)
XBL767-3109

Fig. 24

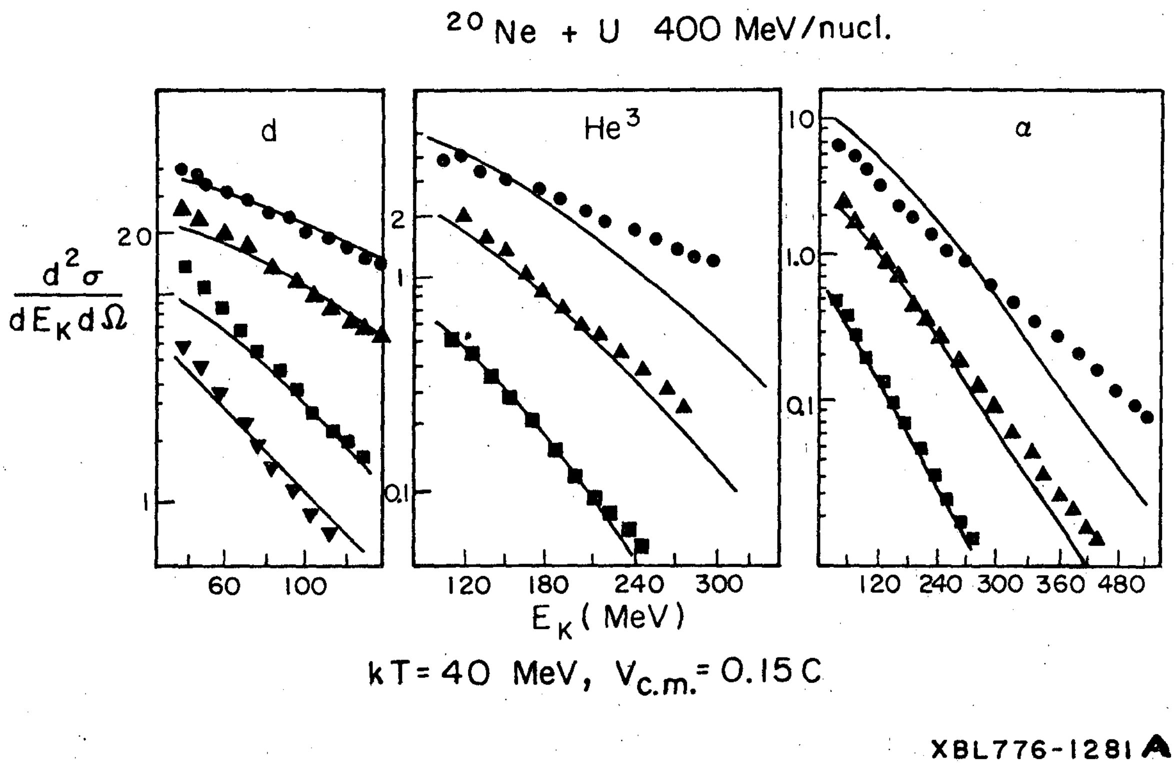

20 Ne + U 400 MeV/nucl.
d
He 3
α
d 2 σ / d E K d Ω
20
1
2
1
0.1
10
1.0
0.1
60
100
120
180
240
300
120
240
300
360
480
E K (MeV)
kT = 40 MeV, V c.m. = 0.15 C
XBL776-1281 A

Fig. 25

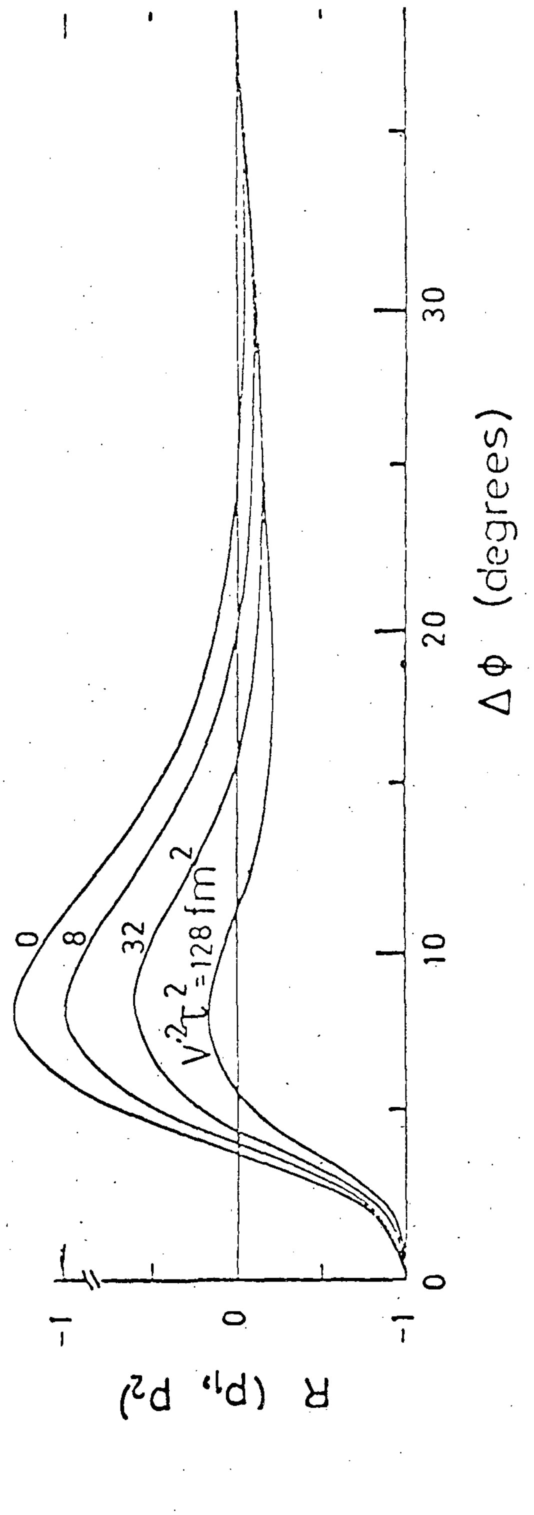

XBL 778-2623

Fig. 26

TECHNICAL INFORMATION DEPARTMENT
LAWRENCE BERKELEY LABORATORY
UNIVERSITY OF CALIFORNIA
BERKELEY, CALIFORNIA 94720